

Metallurgical Research on Glass-to-Metal Seals



Don Susan

Joining and Coatings Dept. 1813
Sandia National Laboratories
Albuquerque, NM

New Mexico Tech, Socorro, NM
Seminar Class
February 6th, 2008

Sandia is a multiprogram laboratory operated by Sandia Corporation, a Lockheed Martin Company,
for the United States Department of Energy's National Nuclear Security Administration
under contract DE-AC04-94AL85000.



Many collaborators make this research possible

Sandia National Laboratories

Mark Reece
Chuck Walker
Alice Kilgo
Paul Hlava
Charlie Robino
Joe Michael
Bonnie McKenzie
Mark Rodriguez
Tom Buchheit
Rajan Tandon

Jill Glass
Sandy Monroe
Ron Stone
Jamey Bond
Dave Goy
Christine Roth
Jim Van Den Avyle
Rob Sorensen
Jeff Christensen

Chad Watson – Boise State University, Boise, ID
Jeff Rodelas – Missouri University of Science and Technology,
Rolla, MO
Matt Perricone – R.J. Lee Group, Pittsburgh, PA
Jim Emmons and Wayne Tuohig – Honeywell, Kansas City Plant



Outline

1. Applications of Glass/Metal Seals

2. Seals with connector shells

2.A. Stainless steel pre-oxidation and seal processing

- Sessile drop testing and characterization results
- Effects of stainless steel composition on seal integrity

2.B. Surface alloy depletion and phase transformations

- Alternative alloys

3. Seals with connector pins

• Glass-ceramic to metal seals

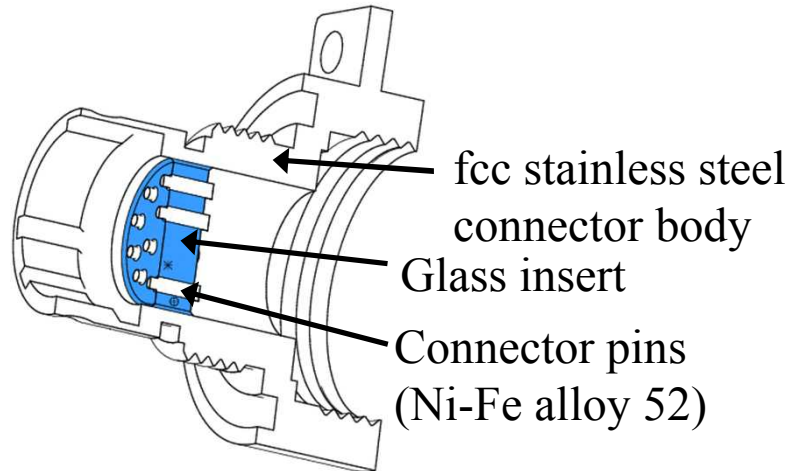
- In-situ pin hardening and metallurgical response of precious metal contact alloys

4. Summary



Sandia Applications – Hermetic Connectors

- Glass-to-metal (GtM) seals must provide a hermetic barrier in high-reliability connectors. “Compression” type seals – outer SS shell with a high CTE, glass with a low CTE, and low-expansion pin material (with CTE approximately matching the glass.)
- Good chemical adhesion is also required between the glass and metal, through the formation of a transitional oxide layer. This layer is provided by “pre-oxidation” of the stainless steel prior to glass/metal joining.

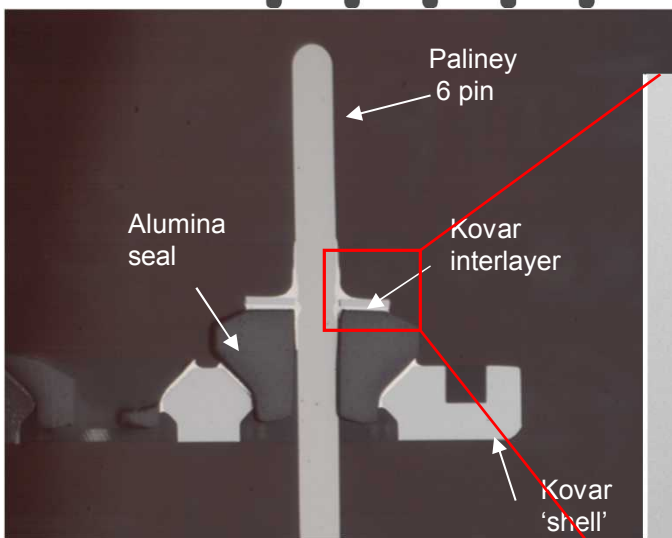
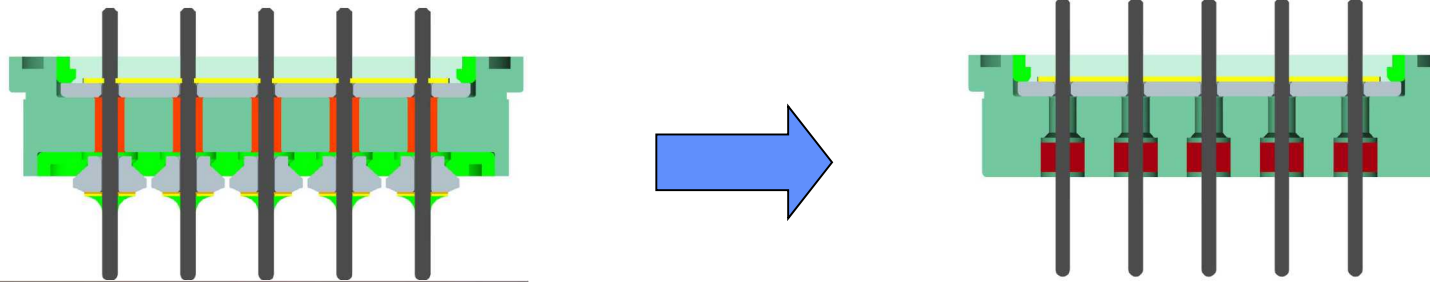
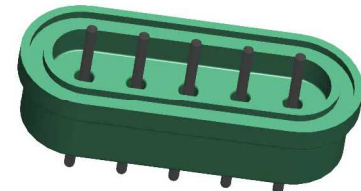


Examples of good vs. poor glass adherence

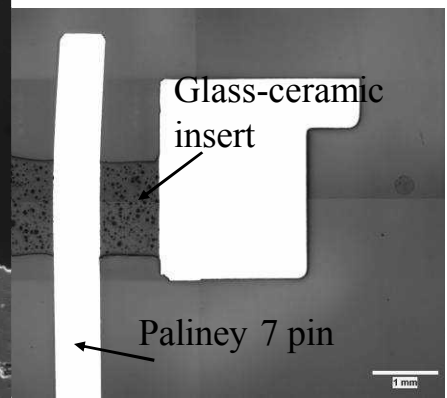
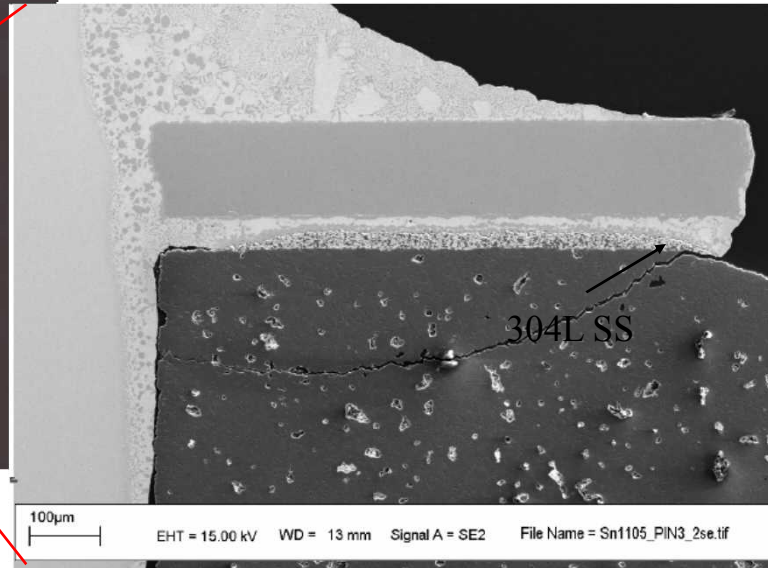


Sandia Applications - Replacement of Brazed Assemblies

- Glass-ceramic/metal seals are being designed to replace complex and expensive brazed assemblies
- Brazed assemblies are strong in axial direction but relatively weak in transverse loading, also difficult to inspect
- Glass-ceramics are robust in high T and P environments (compared to conventional glass seals)



Optical micrograph of cross-sectioned brazed Alumina hermetic seal

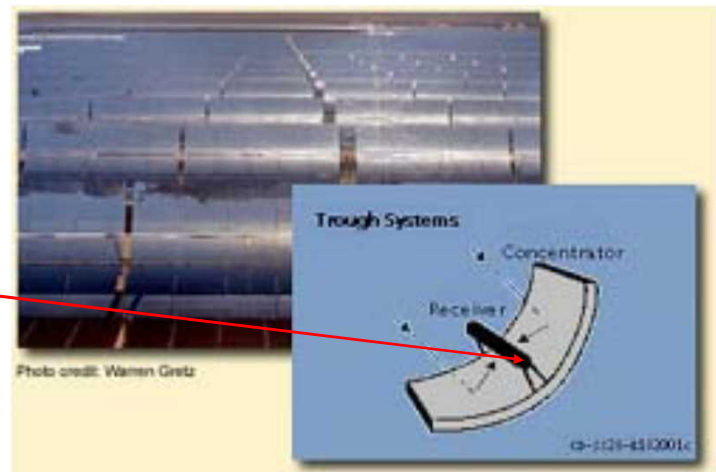
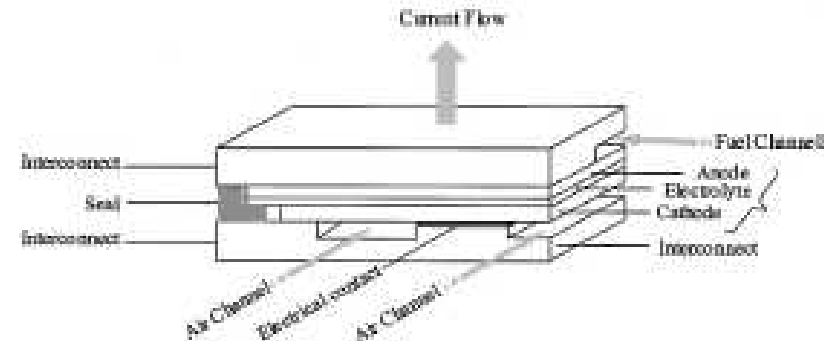


Cross-sectioned glass-ceramic-to-metal seal



Other Applications

- Fuel cells
 - Seal to ferritic stainless steel and ceramic/composite layers for hermeticity
- Parabolic solar concentrators
 - Glass tube with heated fluid, sealed to 316 SS

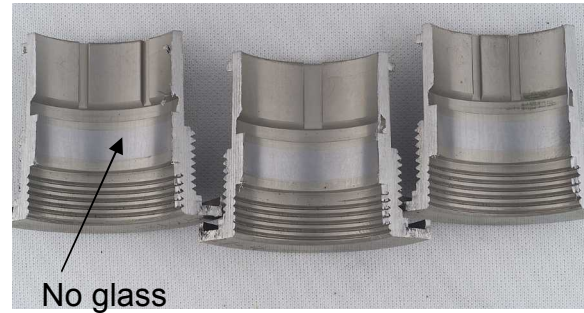




2.A. Pre-oxidation and glass sealing (connector shells)



Examples of good vs. poor glass adherence



Schematic of chemical bonding in metal/oxide/glass interface

**Pre-oxidation generally performed to provide transition layer.
Oxidation and bonding require diffusion processes**

Observed glass bead
fracture interface



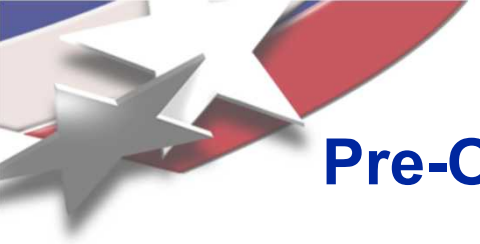
Metal

Metal Oxide Layer

Glass

Table 2 Thermal expansion coefficient of oxides and stainless steels

Material	Coefficient ($10^{-7}/^{\circ}\text{C}$)	Temperature range
SiO_2 (amorphous)	5.0	20–500°C
SiO_2 (α Quartz)	193.5	20–500°C
Cr_2O_3	84.3	20–500°C
Fe_2O_3	113.6	20–500°C
STS430LX	115.0	20–500°C
STS304	183.0	20–500°C



Pre-Oxidation and Glass/Metal Seal Processing

- Analyzed several heats of 304L and 316L
- Pre-oxidation of stainless steel:
 - 1000, 1050, and 1095°C
 - 30 and 90 minutes, cool to room temp.
 - Low pO_2 atmosphere, to avoid Fe oxidation
- GtM sealing:
 - 920 to 970°C, ~15 minutes, N_2/H_2 atmosphere, cool to room temp.

- Pre-oxidation produces thin oxide with Cr_2O_3 , $MnCr_2O_4$, and SiO_2 phases.
- Provides transitional layer with bonding to both the metal and the glass

Glass/304L Seal Behavior Appeared to be “Heat Lot Specific”

Pre-oxidation
conditions

1000°C/30 min

1000°C/90 min

1050°C/30 min

1050°C/90 min

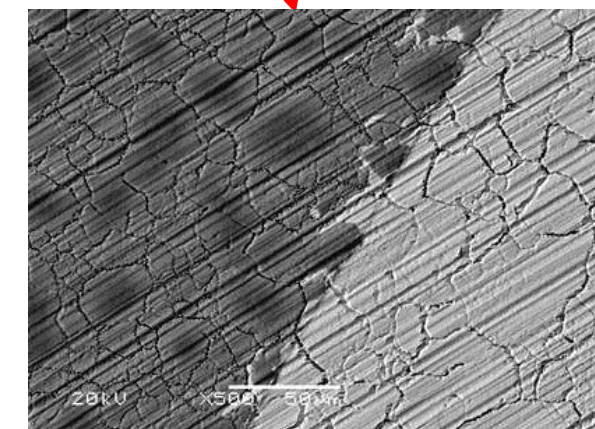
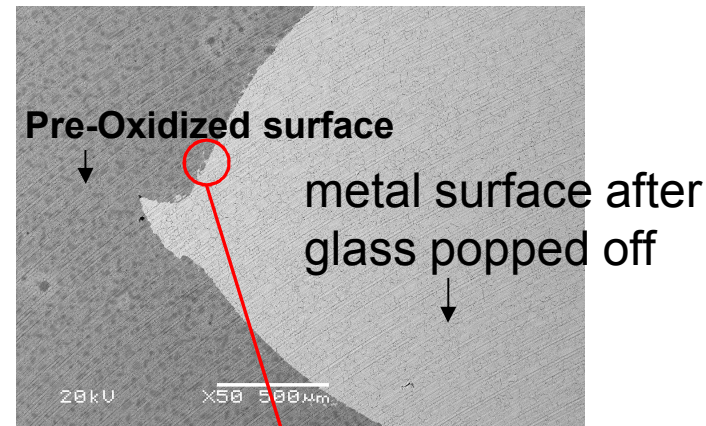
1095°C/30 min

1095°C/90 min

A B C D



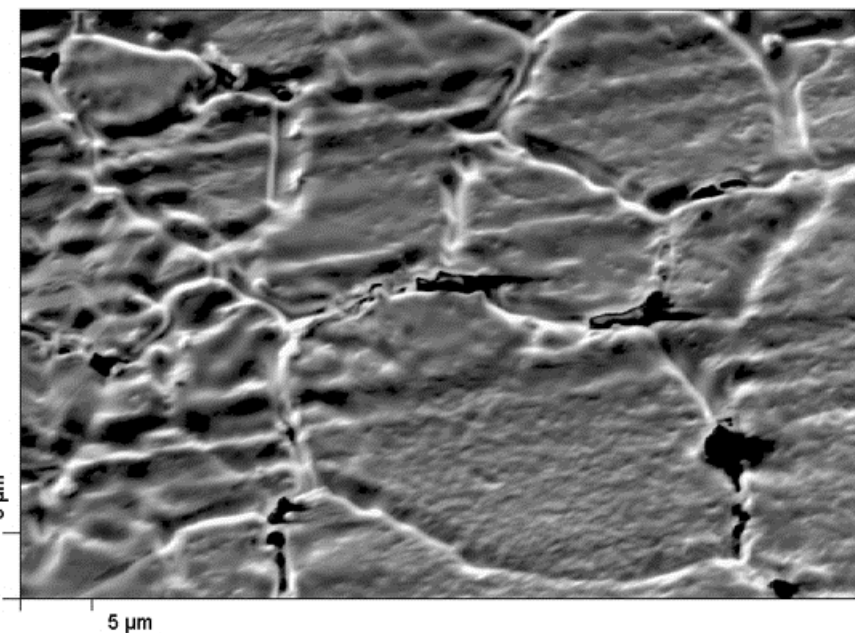
Glass sessile drop
conditions were the same
for all samples.





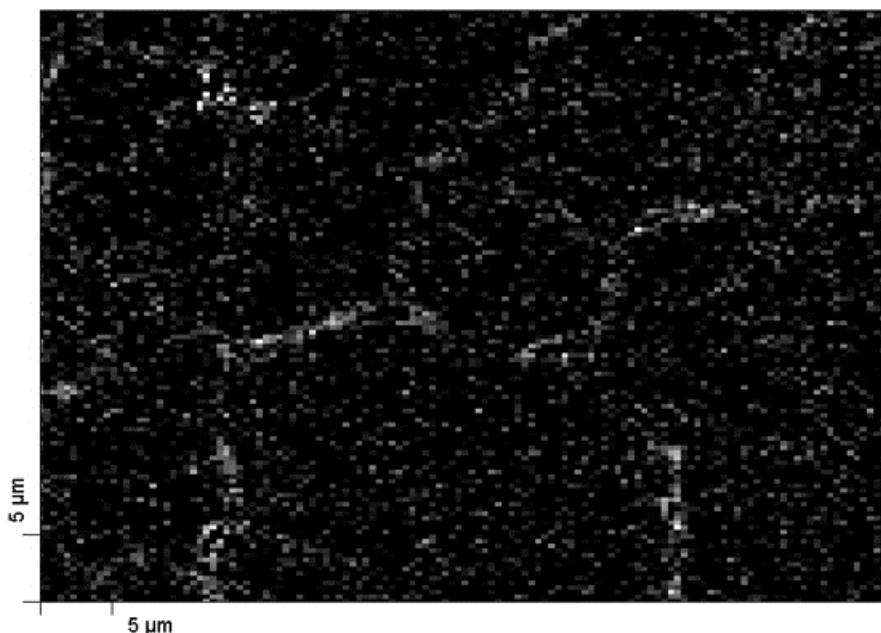
Metal Side, 1050°C/30 min Region of Glass Bead Debonding

SEM



Secondary Micrograph

Si2



Silicon EDS Elemental Map

Si in grain boundaries
Grain boundary “etching”

Literature on Oxidation of Austenitic Stainless Steel

Ni Plate



Fig. 11. Backscattered SEM micrograph of the cross-section of oxide formed on RS1.5 after 300 hr of cyclic oxidation in pure O₂ at 900°C.

1.5 wt. % Si
+ small grain size, no sulfur

Ni plate

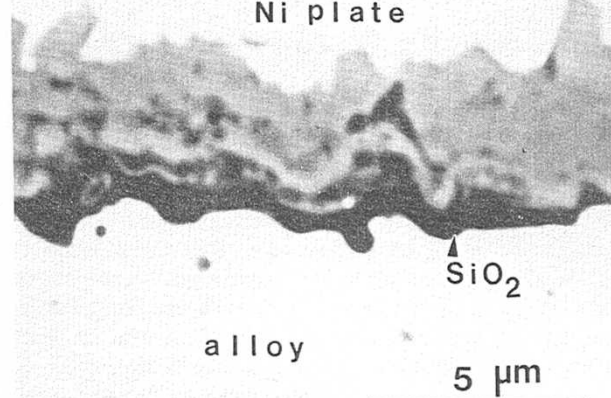


Fig. 14. (a) SEM micrograph of oxide formed on RS1.5MnS after 300 hr of cyclic oxidation in pure O₂ at 900°C, in cross-section. There is a zone in the alloy that is denuded of MnS precipitates. (b) Higher magnification backscattered SEM micrograph showing the continuous silica layer between the alloy and the external duplex layer.

1.5 wt. % Si
+ sulfur (MnS) + small grain size

Continuous SiO₂ layer,
slower oxidation kinetics

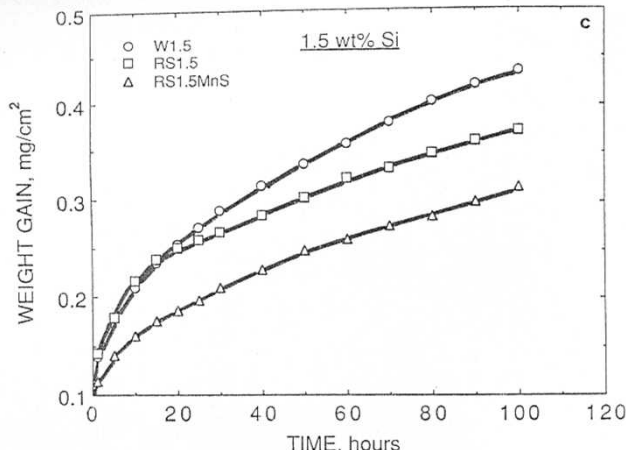
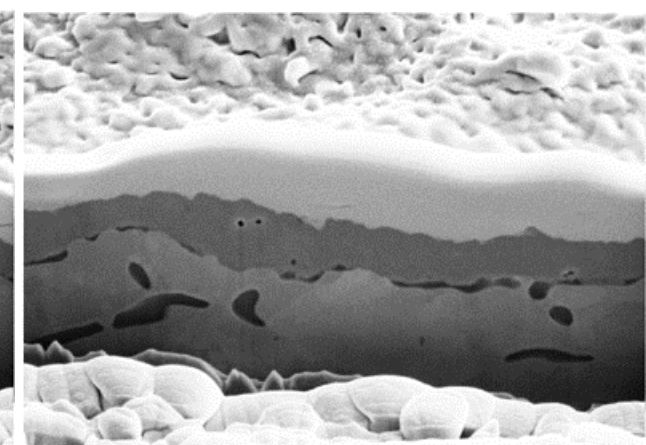
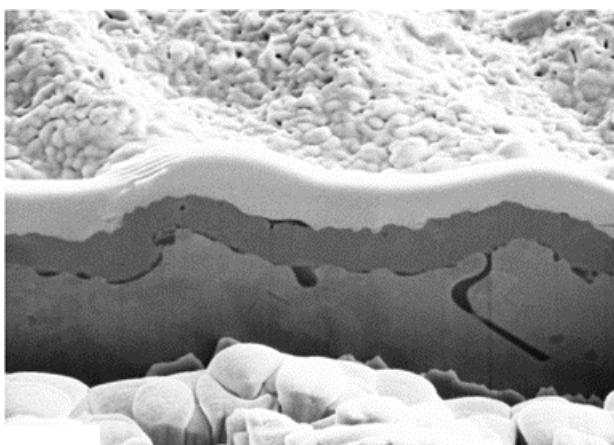
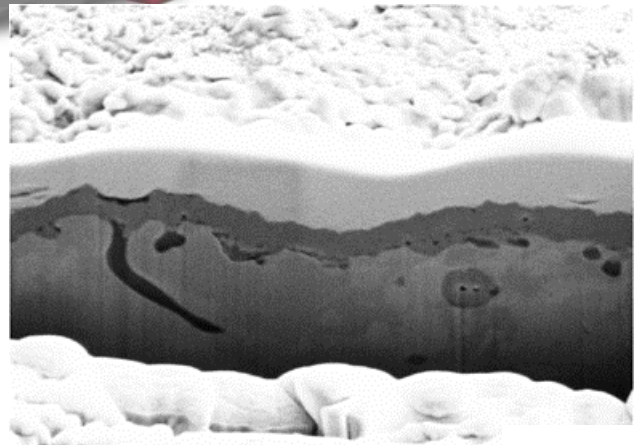


Fig. 15. Continued.

(Basu, S.N. and G.J. Yurek, *Effect of Alloy Grain Size and Silicon Content on the Oxidation of Austenitic Fe-Cr-Ni-Mn-Si Alloys in Pure O₂*. Oxidation of Metals, 1991. 36(3/4): p. 281-315.)

FIB Cuts and TEM: “Good” Oxide Morphology (and Chemistry)

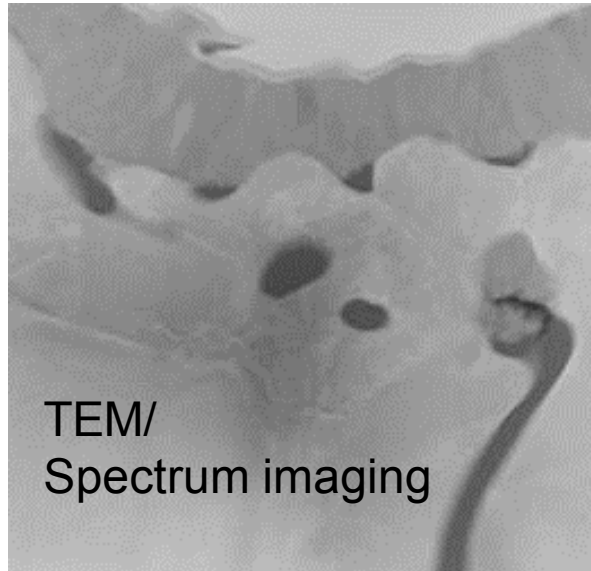


SEM/FIB

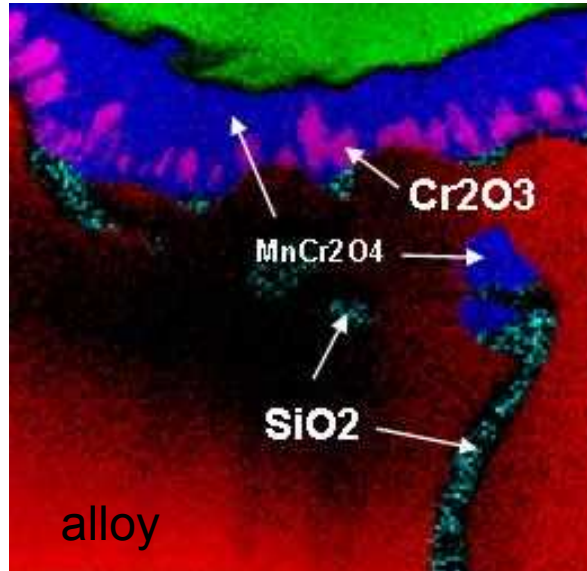
E-Beam 5.00 kV Det SED Spot 3 FWD 5.092 Tilt 52.0° Scan H 22.63 s Mag 15.0 kX 2 μm

E-Beam 5.00 kV Det SED Spot 3 5.033 FWD Tilt 52.0° Scan H 22.63 s Mag 15.0 kX 2 μm

E-Beam 5.00 kV Det SED Spot 3 FWD 5.024 Tilt 52.0° Scan H 22.63 s Mag 15.0 kX 2 μm



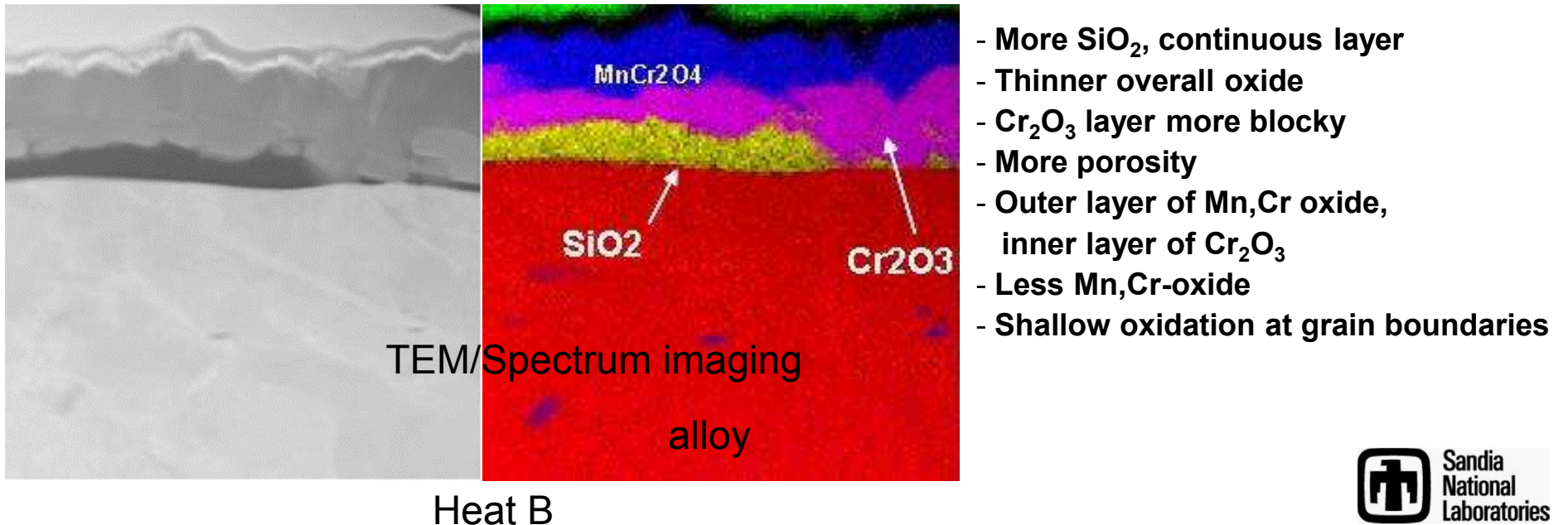
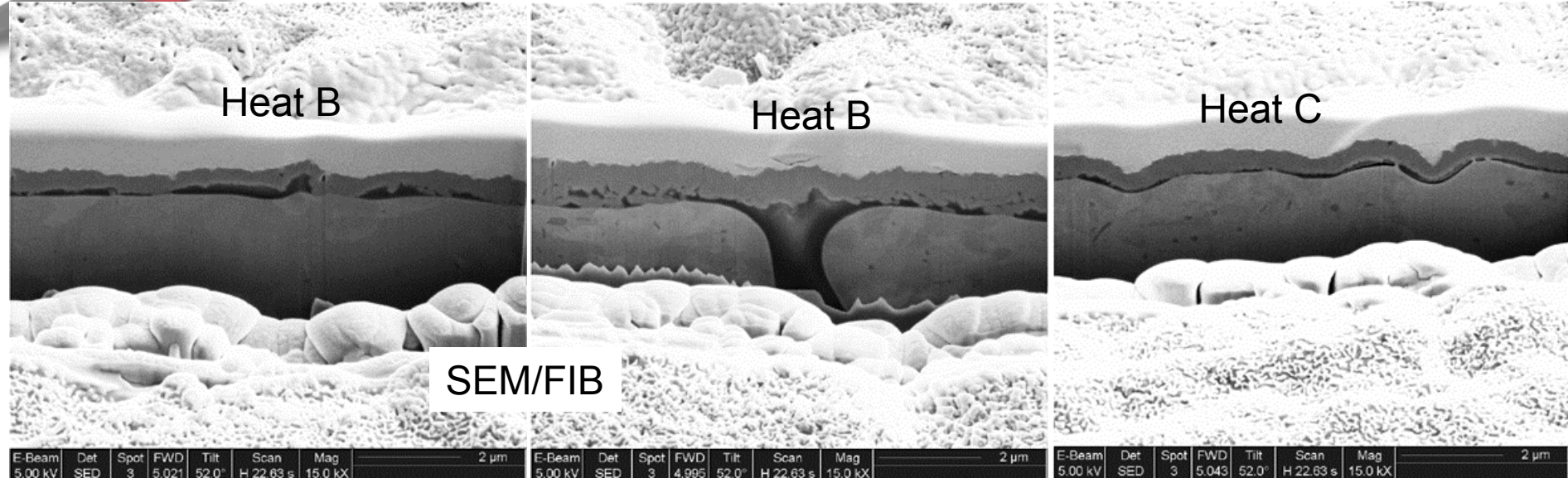
TEM/
Spectrum imaging

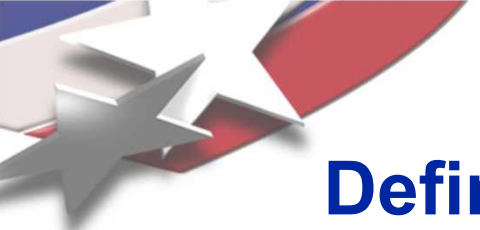


Heat A

- Thicker overall oxide
- Dense oxide, ~ little porosity
- More Mn-containing oxide
- Inner Cr_2O_3 not fully continuous
- SiO_2 less continuous, less coverage
- Oxidation along alloy grain boundaries

FIB Cuts and TEM: “Poor” Oxide Morphology (and Chemistry)





Define oxide layer characteristics that provide good glass wetting and adhesion

- Columnar, dense oxide grains with low porosity. Rough/convoluted oxide/alloy interface (not smooth)
- Minimal length and fraction area coverage of SiO_2 interface phase
- Maximize fraction of MnCr_2O_4 oxide spinel phase
- Adequate thickness so some oxide remains after glass bonding

Good behavior, 1050°C 30 min. preox. and glassed

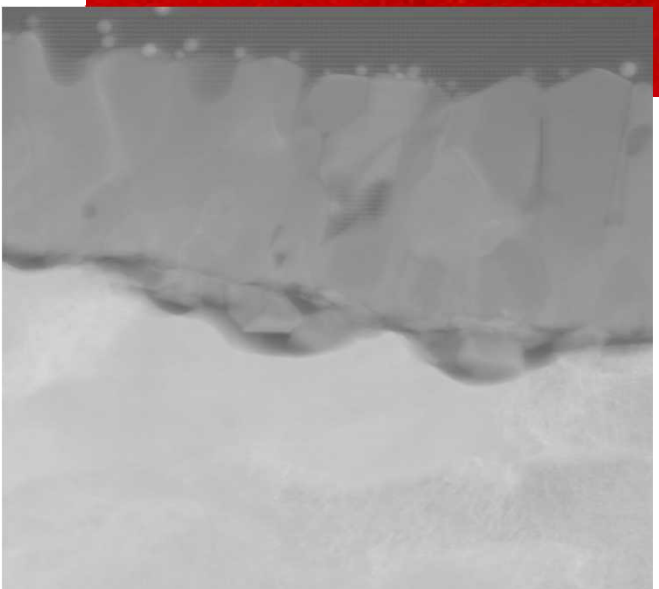
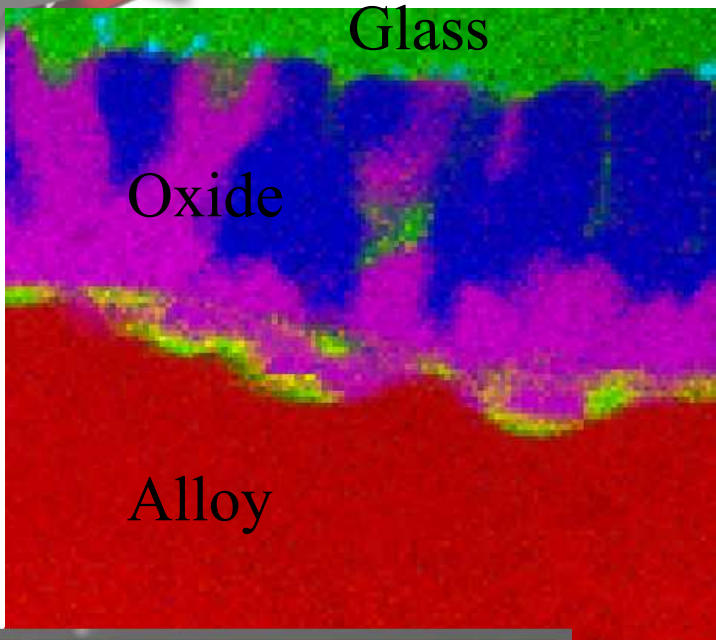
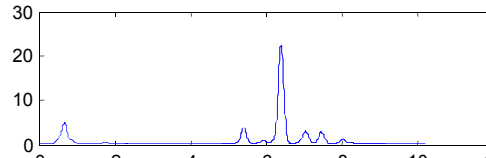
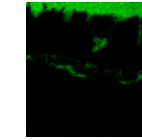
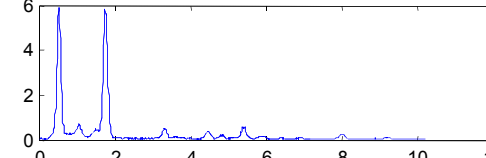


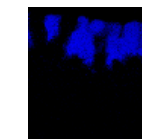
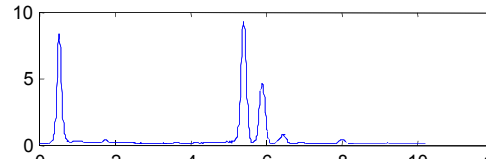
Image width = 1500 nm



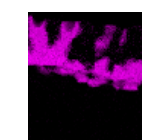
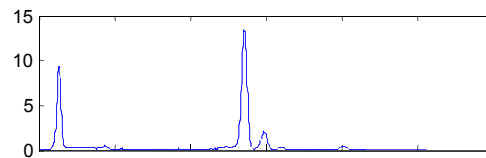
Fe, Cr, Ni



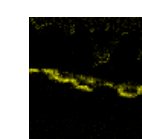
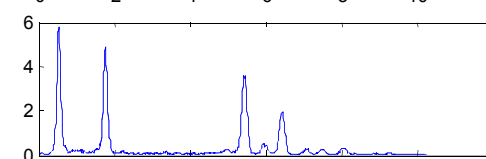
Si, O, K, Ba



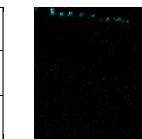
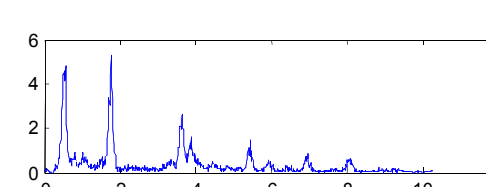
Mn, Cr, O



Cr, O



Si, O



Si, Sb, O

Poor behavior, 1050°C 30 min. preox. and glassed

Non-adherent
glass/metal bond

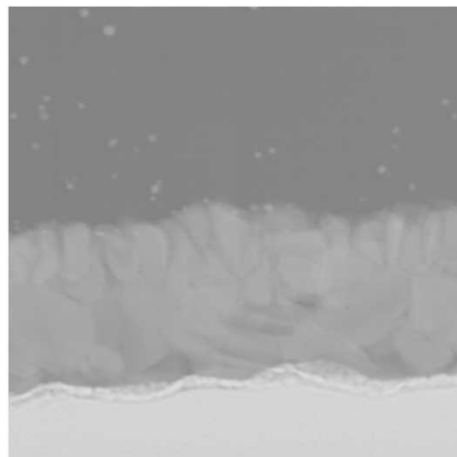
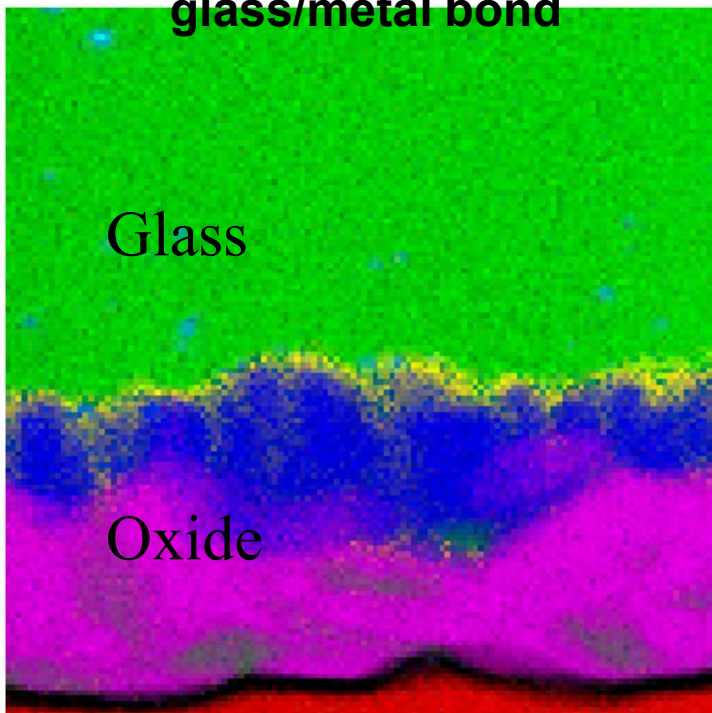
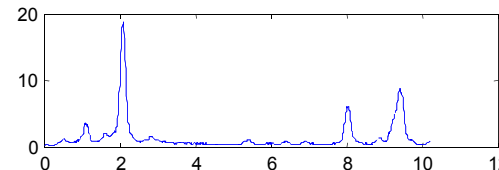
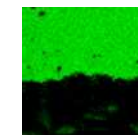
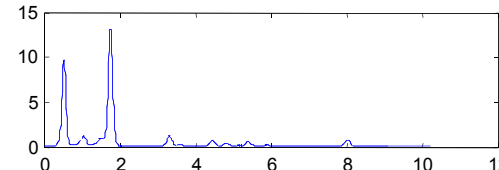


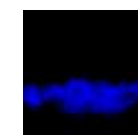
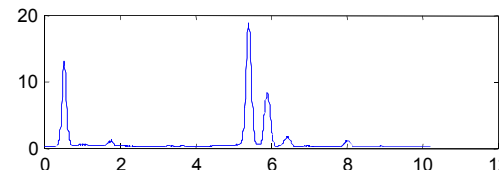
Image width = 1500 nm



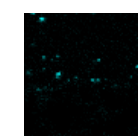
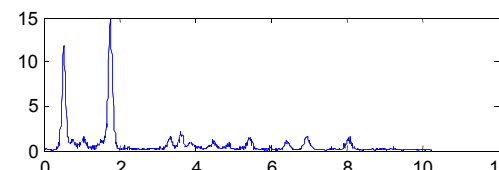
Pt



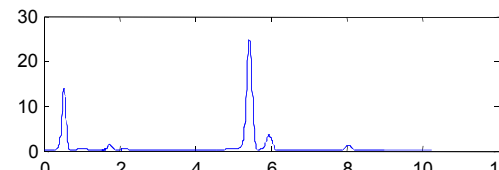
Si, O, K, Ba



Mn, Cr, O



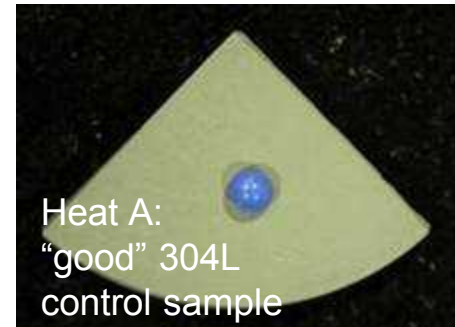
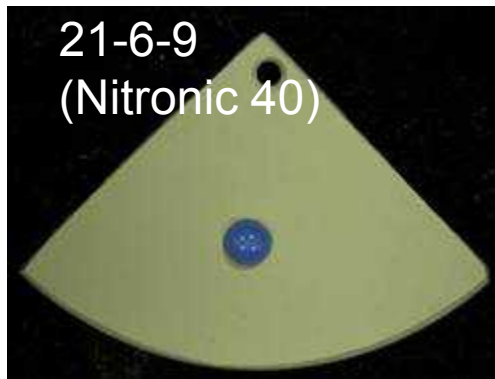
Si, Sb, O



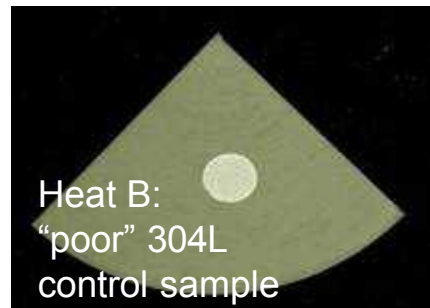
Cr, O

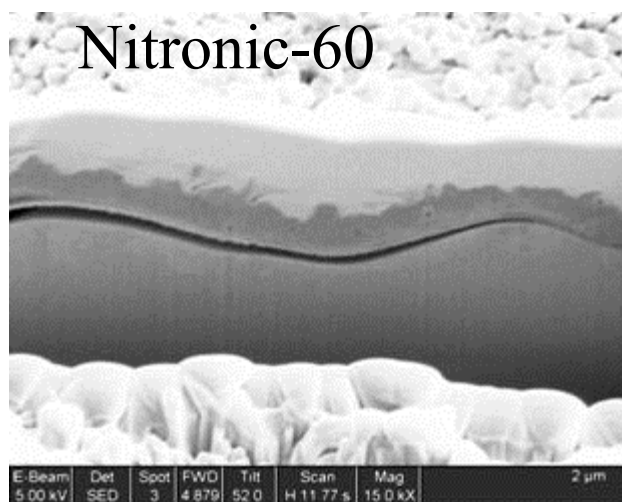
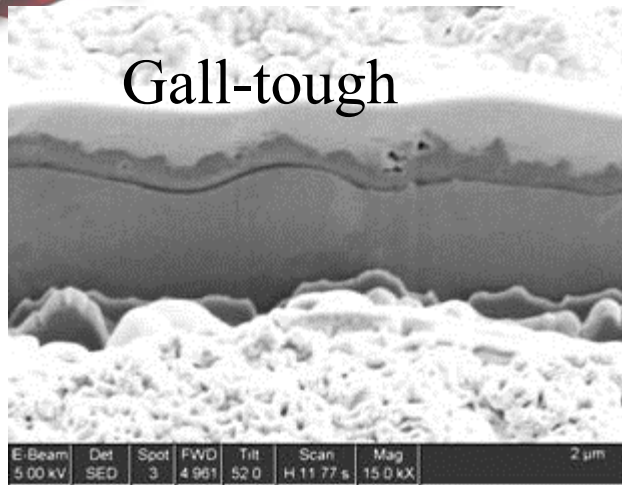


Other Austenitic Stainless Steels



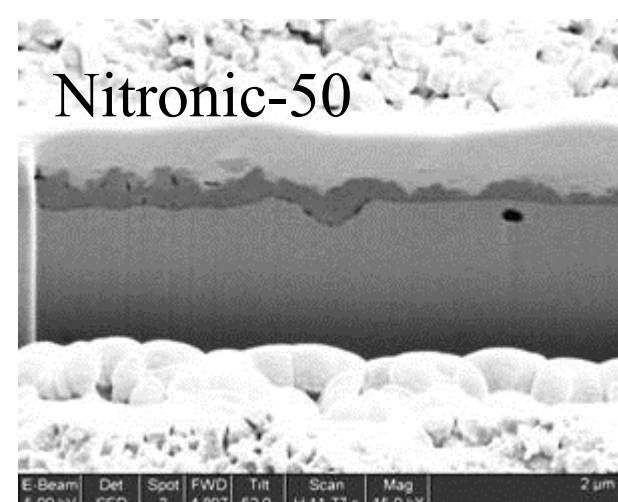
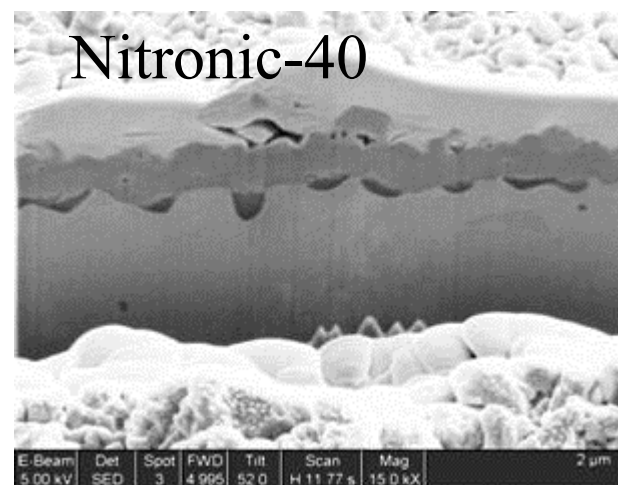
Pre-Oxidation: 1095°C, ~30 min
Sessile drop sealing cycle: same for all samples





Poor glass adhesion

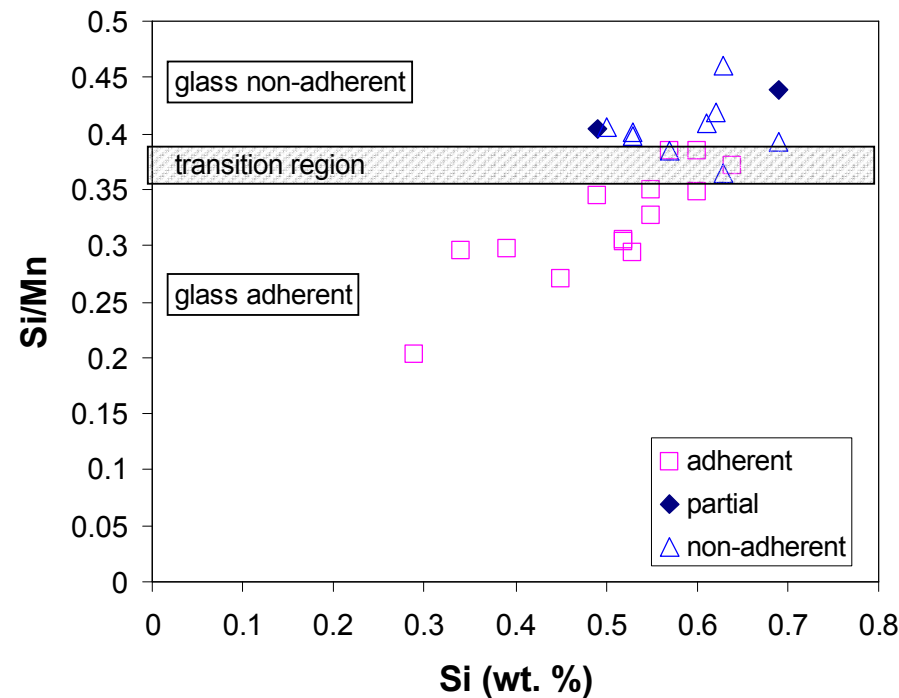
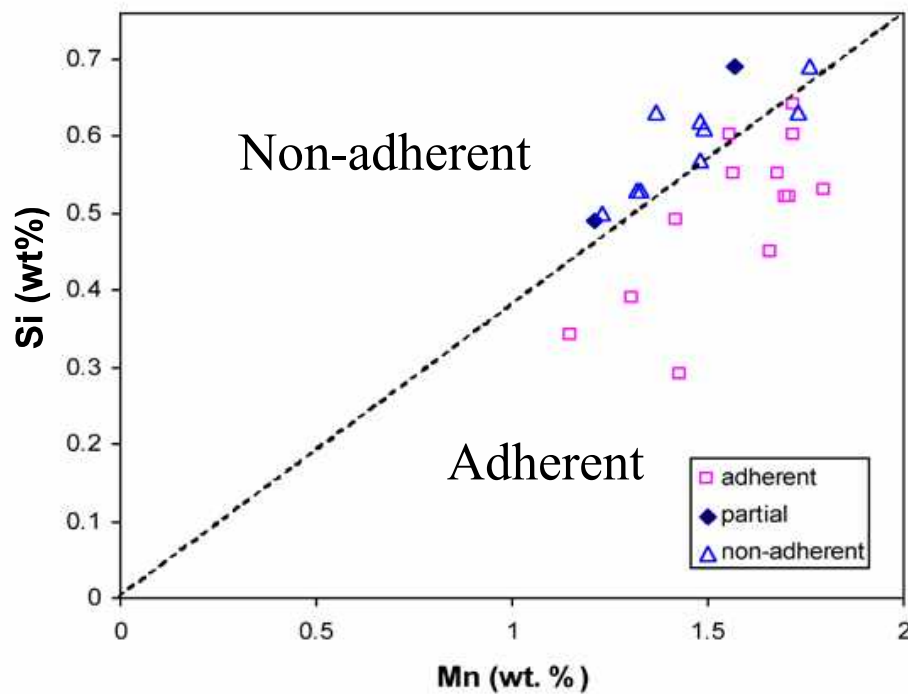
- Oxide morphological requirements appear to hold for other stainless steels as well



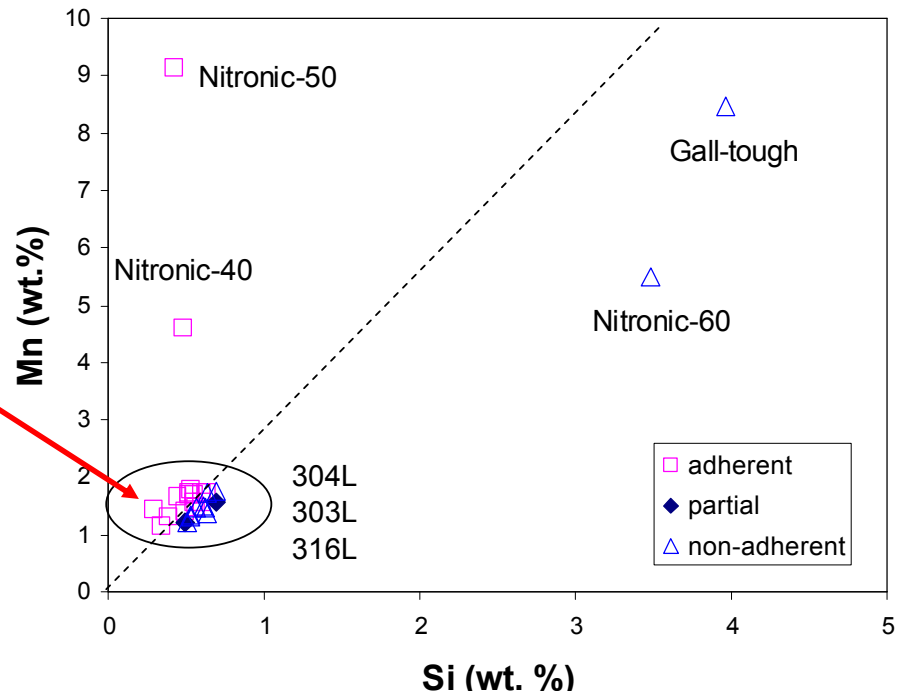
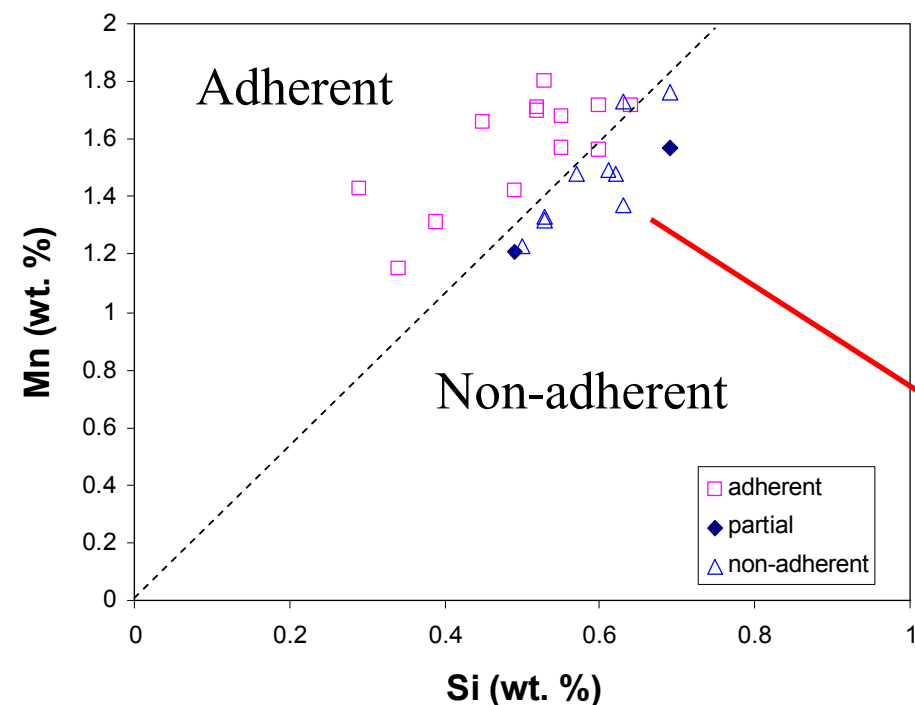
Good glass adhesion

Effect of Alloy Chemistry on Glass Sessile-drop Behavior

- 23 heats identified on this plot
- Si/Mn ratios $> \sim 0.38$ show poor glass adherence, lower ratios show good adherence
- Si and Mn are minor elements in 304L but are strong oxide formers
- Si/Mn ratio could provide a *predictive method* to select heats that will exhibit good glass sealing behavior



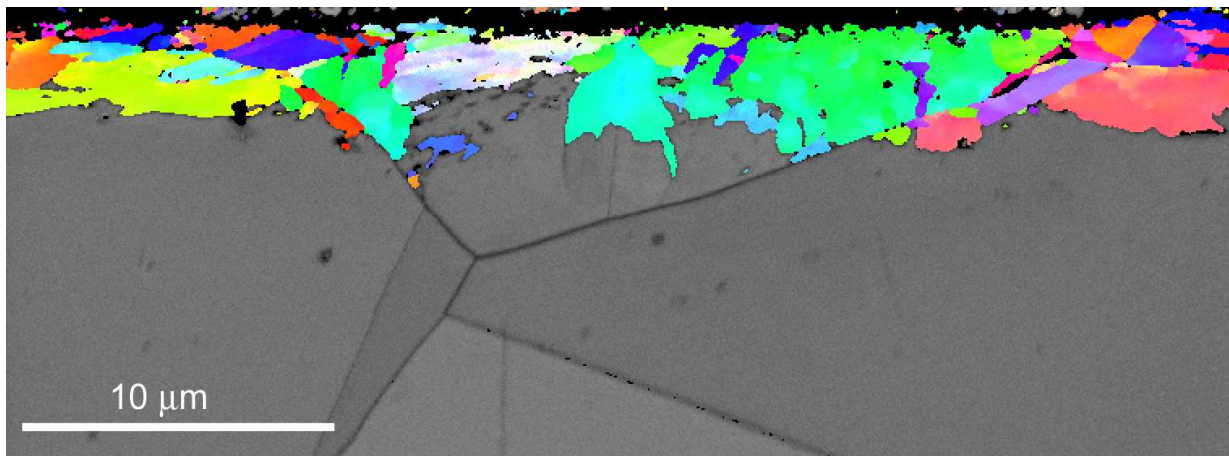
Results for Austenitic Alloys Well-Outside the Range of 304L



- Trends appear to hold for many alloy compositions

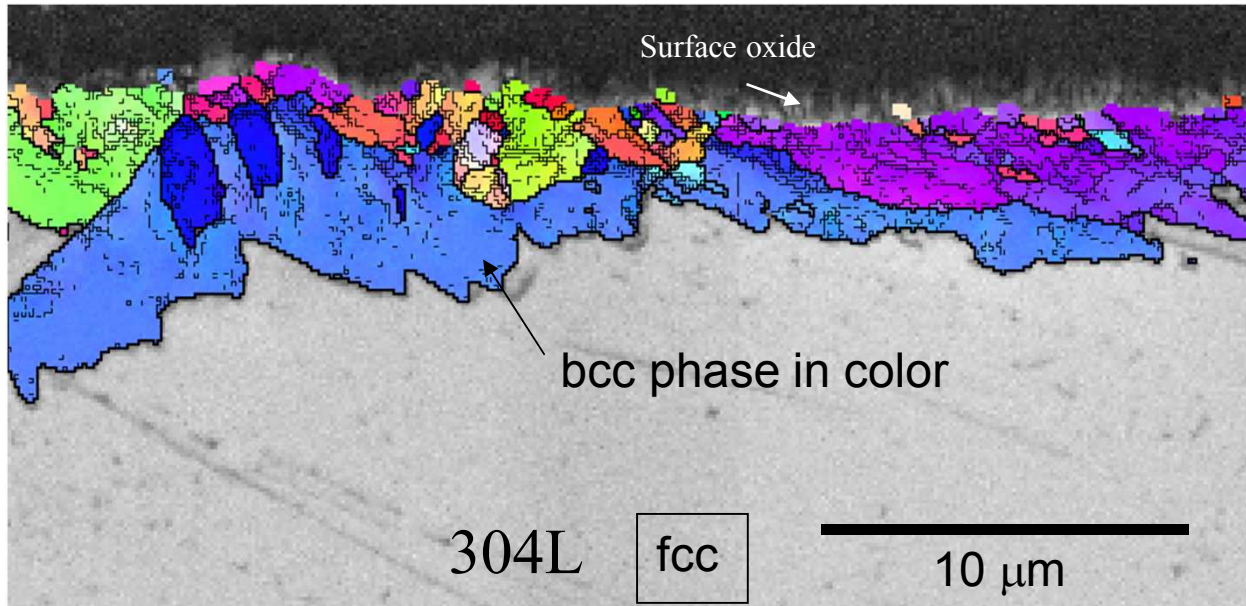


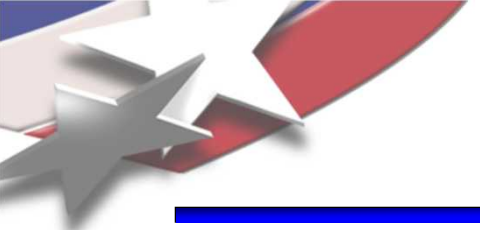
2.B. Surface Alloy Depletion During Pre-Oxidation and Glass Sealing



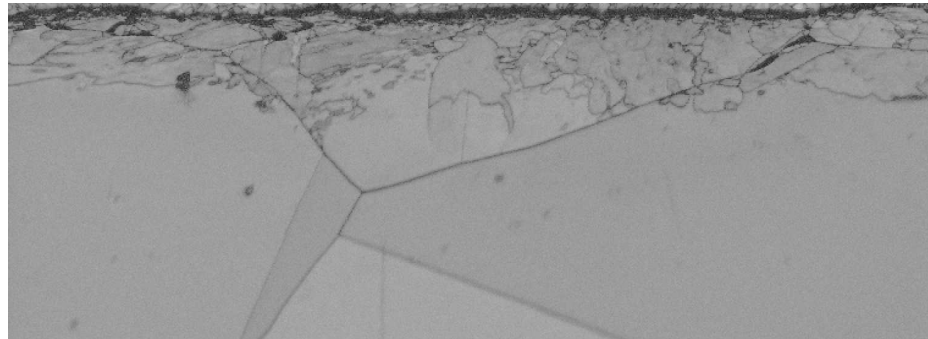
Motivation: Observed a bcc transformed layer near the surface of 304L

- Issues: Phase transformations in the alloy, near the metal/glass interface, could be detrimental to GtM sealing.
 - An fcc-to-bcc transformation produces material with a lower CTE than the bulk austenitic 304L (possible loss of compression seal).
 - The transformation also produces a volume change and possibly high stresses near the glass interface which could result in glass/oxide cracking and/or loss of adhesion.

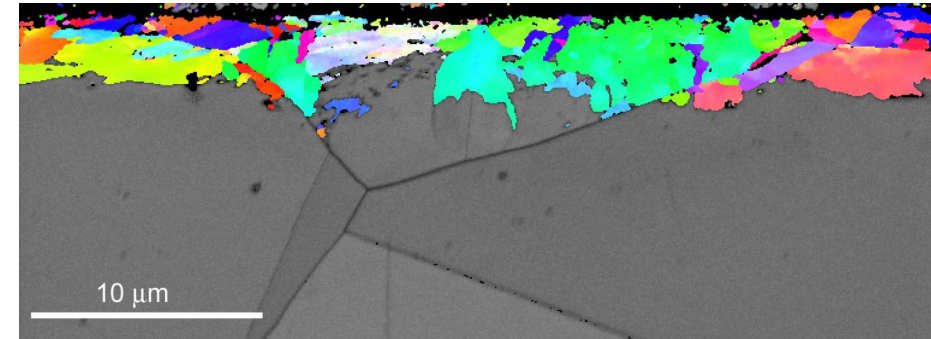




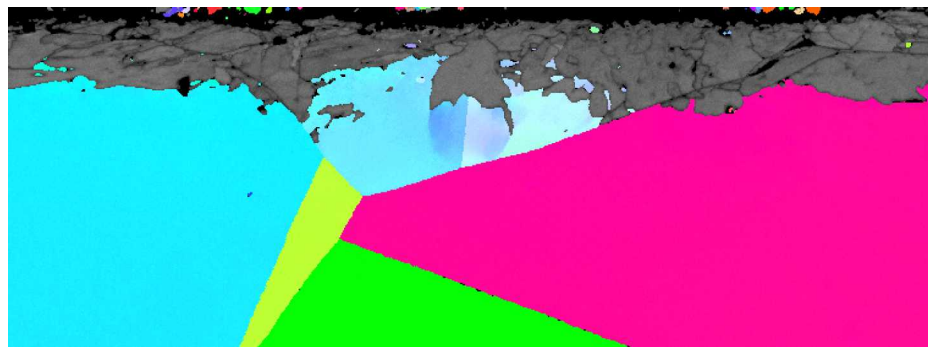
SEM, EBSD Results



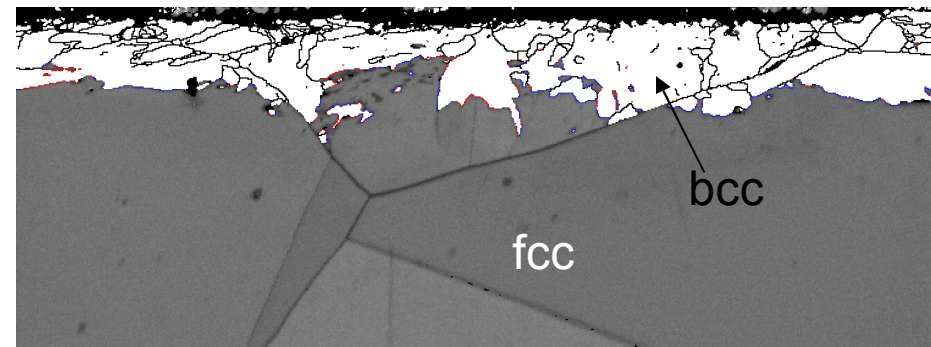
Band Contrast



Ferrite (body-centered)



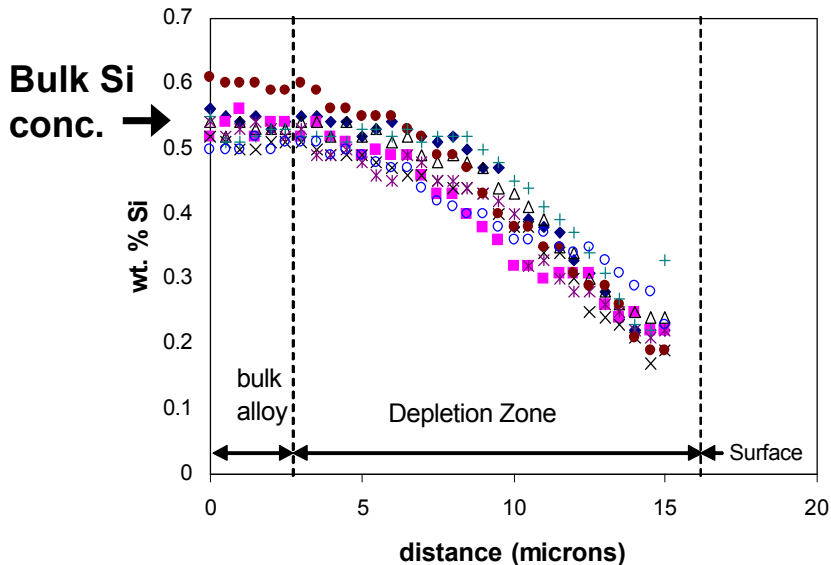
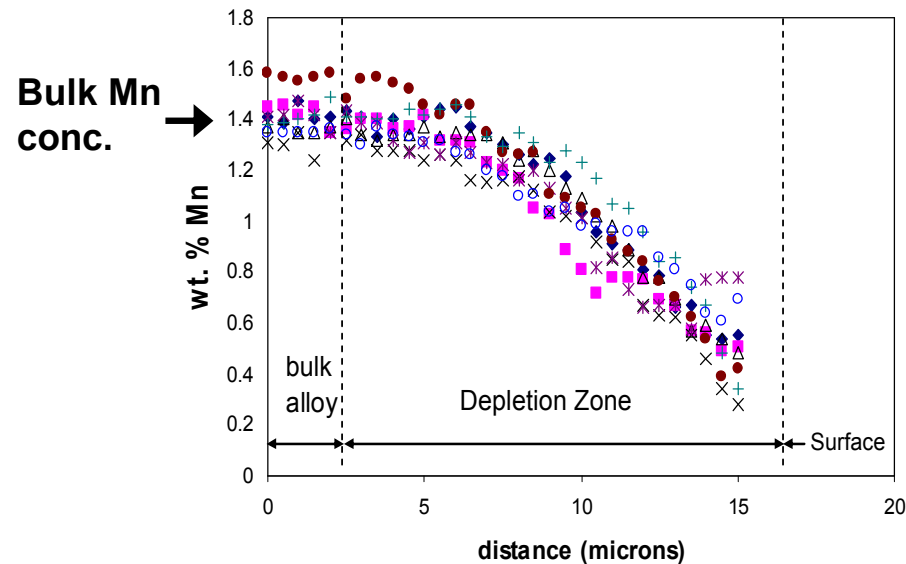
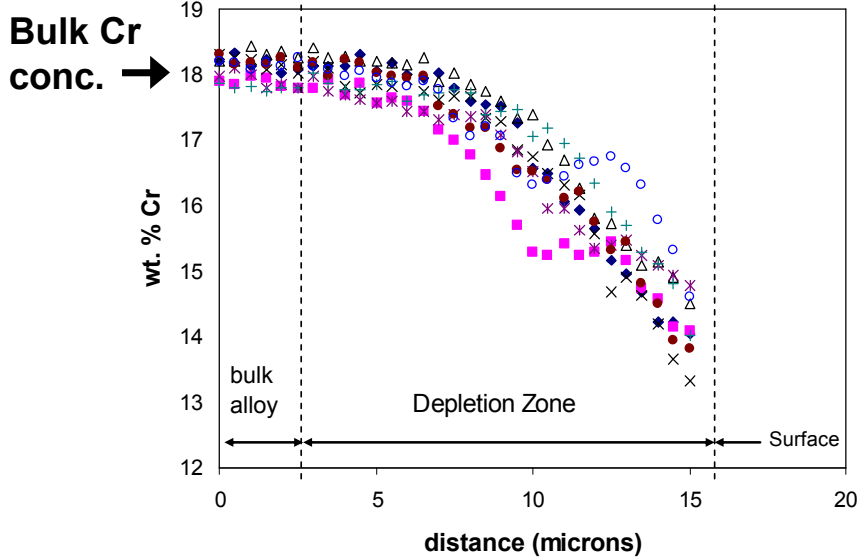
Austenite (fcc)



Kurdjumov-Sachs relationship – blue
Nishiyama-Wasserman relationship - red

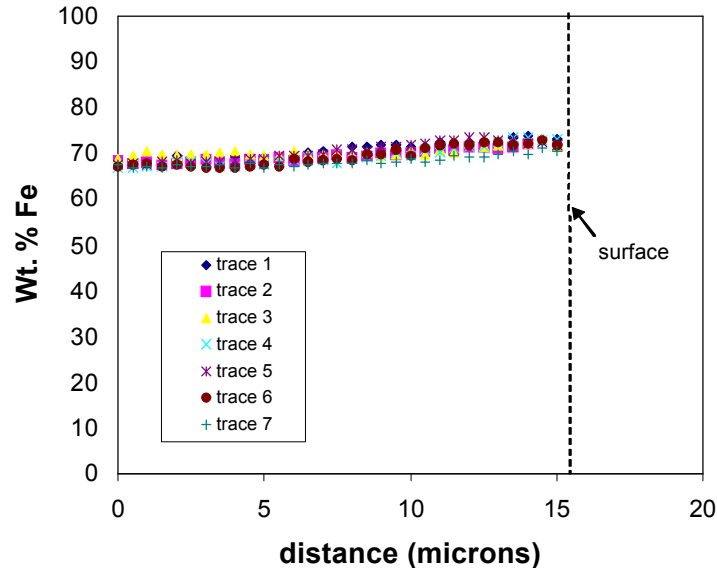
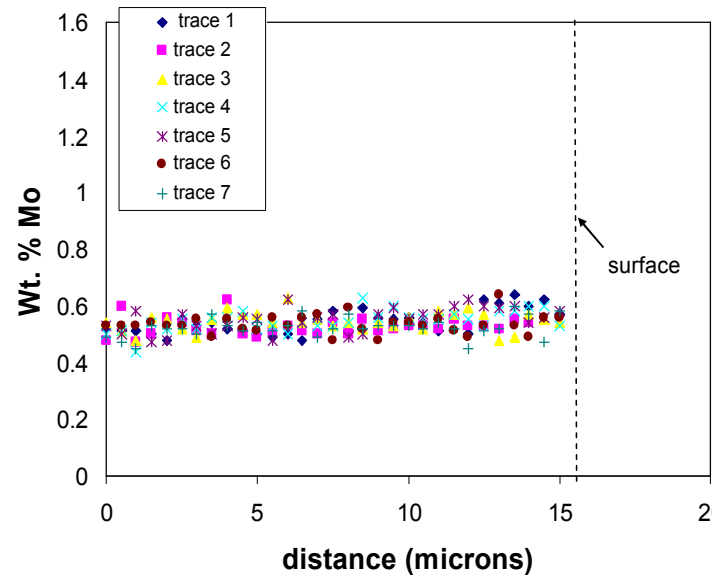
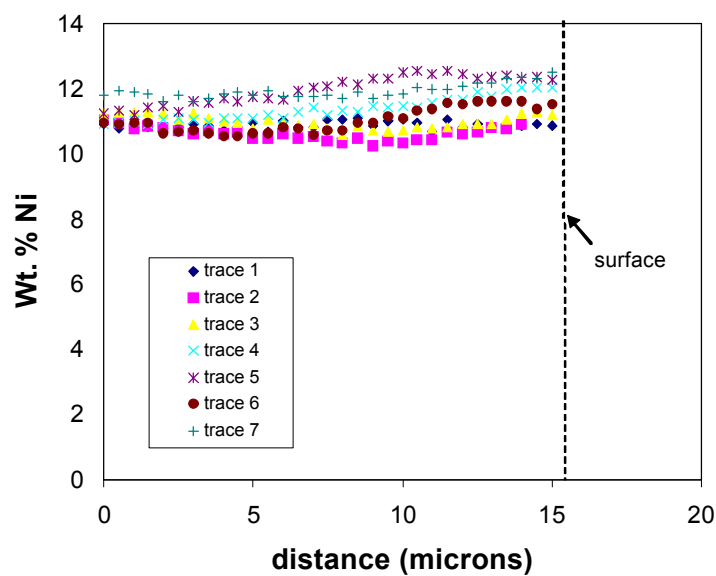
- What causes the fcc-to-bcc transformation near the alloy surface?
- What type of transformation (diffusional, martensitic, etc.)?

EPMA shows alloy depletion near the surface



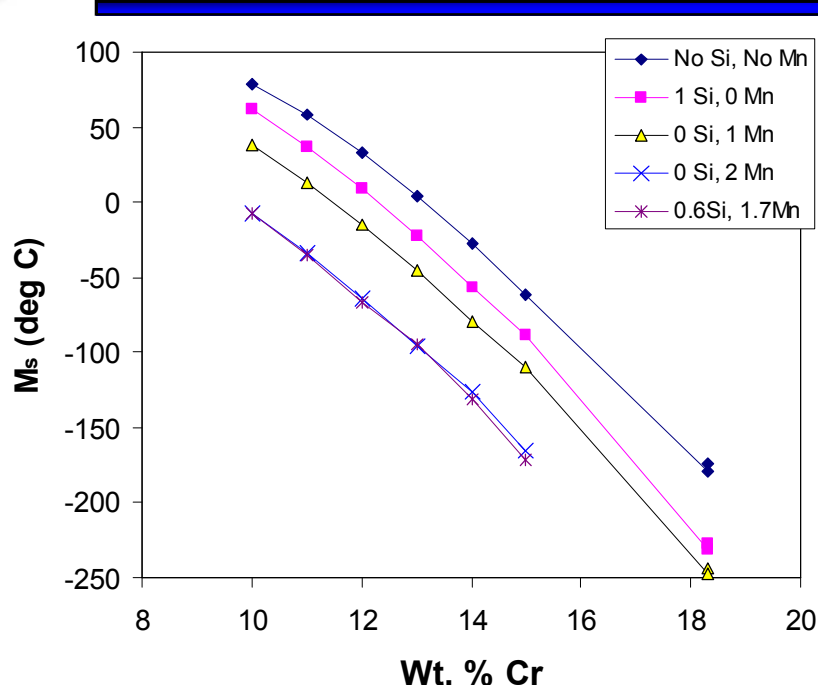
- 1095°C, 30 min. oxidation
- Multiple EPMA traces performed on each sample.
- Significant depletion of the elements Cr, Mn, and Si, *all involved in surface oxidation*. (oxide phases formed on 304L are Cr_2O_3 , MnCr_2O_4 , and SiO_2)

Fe, Ni, and Mo (not involved in oxidation) remain constant or slightly increase near the surface

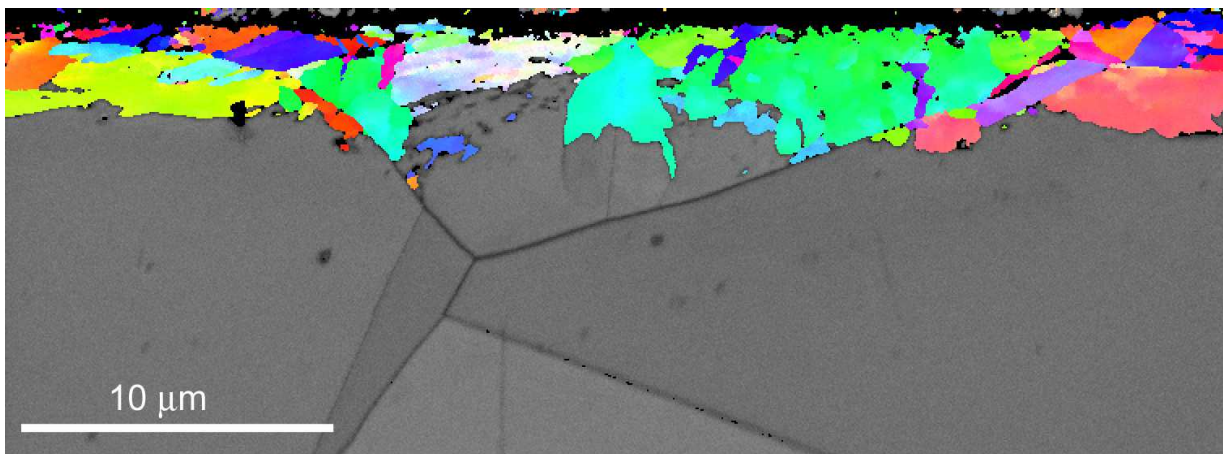


- Low pO_2 oxidation atmosphere avoids Fe oxidation. This also results in an effective slight increase in Fe concentration near the surface
- * Within the resolution of EPMA, no “step” in composition associated with the fcc/bcc interface

JMatPro: Calculated Martensite-start temperature *increases* with Cr Depletion



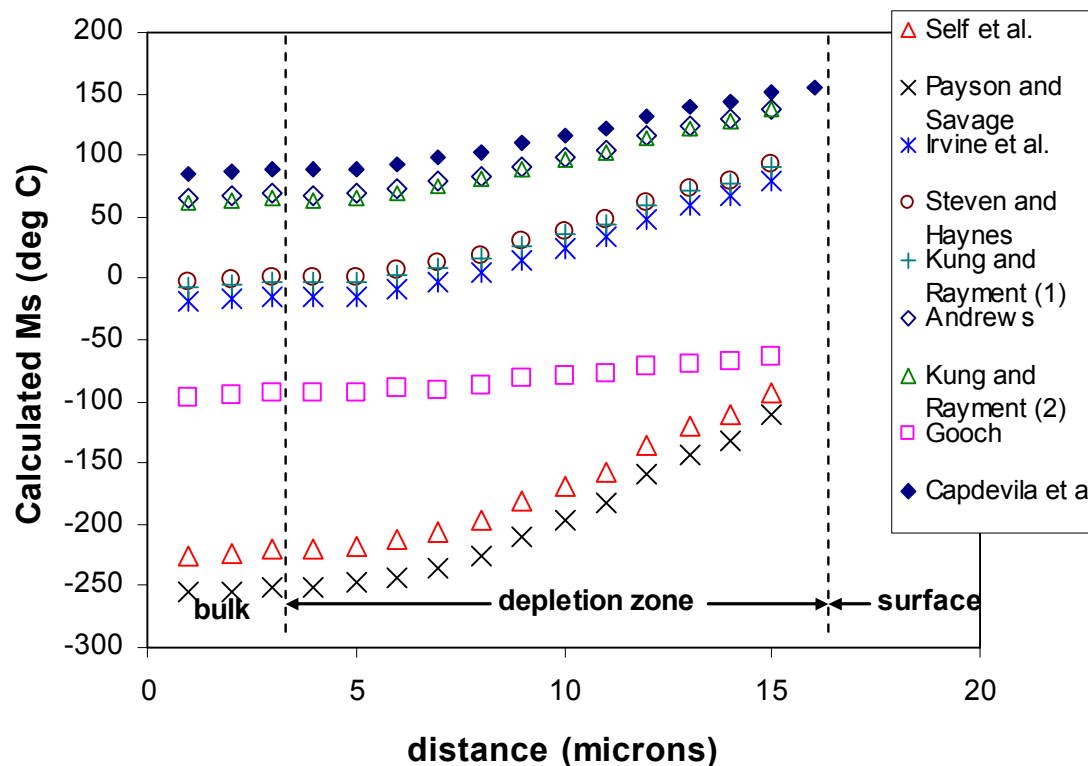
- JMatPro results support a possible martensitic phase transformation in the depletion layer



- Layer morphology and crystallographic orientation relationships also support martensitic reaction

Attempt to correlate the near-surface depletion zone chemistry with M_s temperature

- Several empirical relations available in the literature -- Most were developed for low-alloy steels and may not be useful for M_s prediction in high-alloy stainless steels such as 304L.
- Input EPMA data from the alloy depletion zone into M_s equations



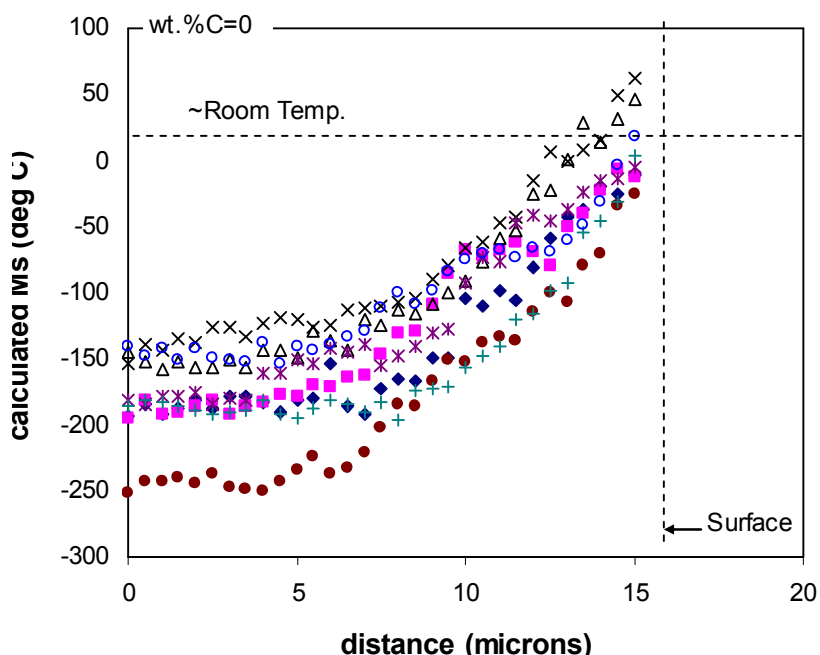
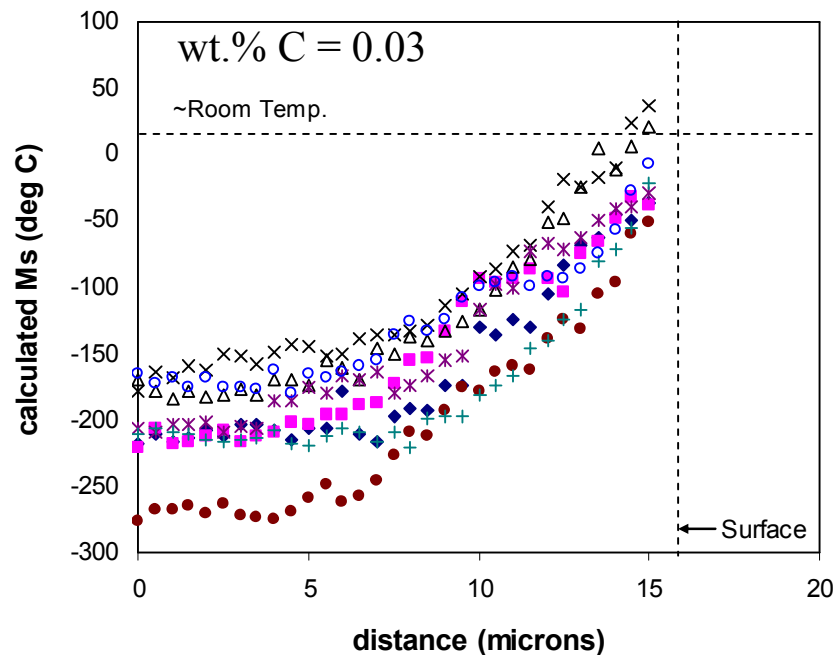
- Either: 1) The bulk alloy M_s temperature prediction is off, or 2) The effect of alloy depletion on M_s temp. does not predict M_s near room temp.

Eichelman and Hull equation - developed for high Cr steels (up to ~18 wt.%): Good correlations for both the bulk alloy M_s and the effects of alloy depletion.

(°F)

$$M_s = 75(14.6 - Cr) + 110(8.9 - Ni) + 60(1.33 - Mn) + 50(0.47 - Si) + 3000(0.068 - [C + N])$$

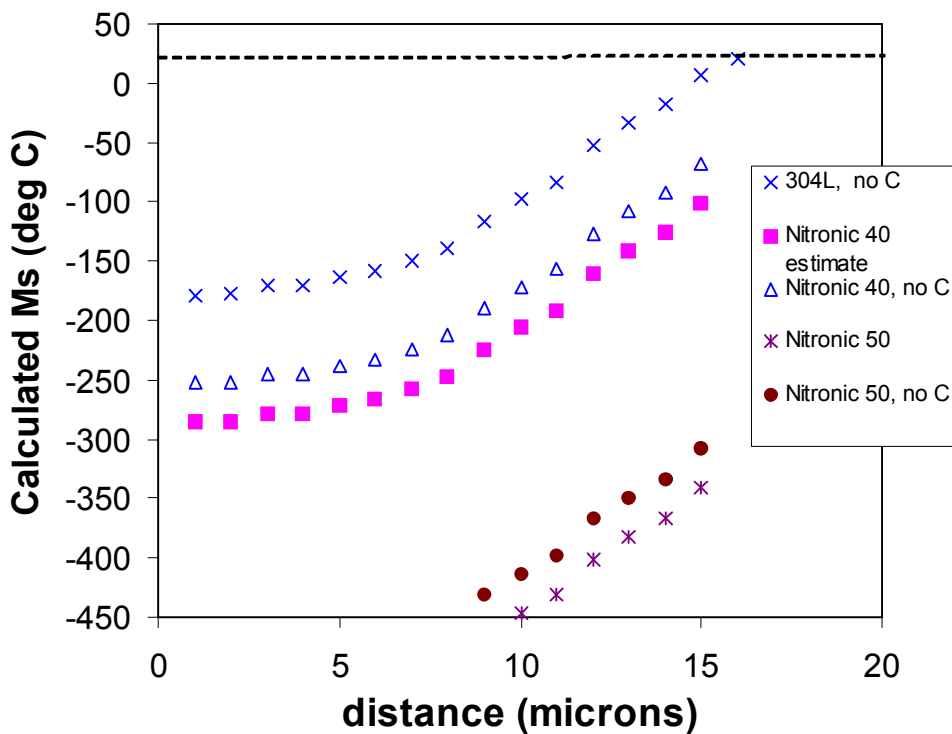
Trans.ASM,
V.45, (1953),
p.77-104



- M_s temperatures at or near room temp. are possible in alloy depletion zone.
(within experimental error of the empirical equation)
- Effect of carbon depletion also considered – calculations with 0% carbon result in slight further increase in M_s .

How can we reduce or avoid martensitic layer formation near the surface ?

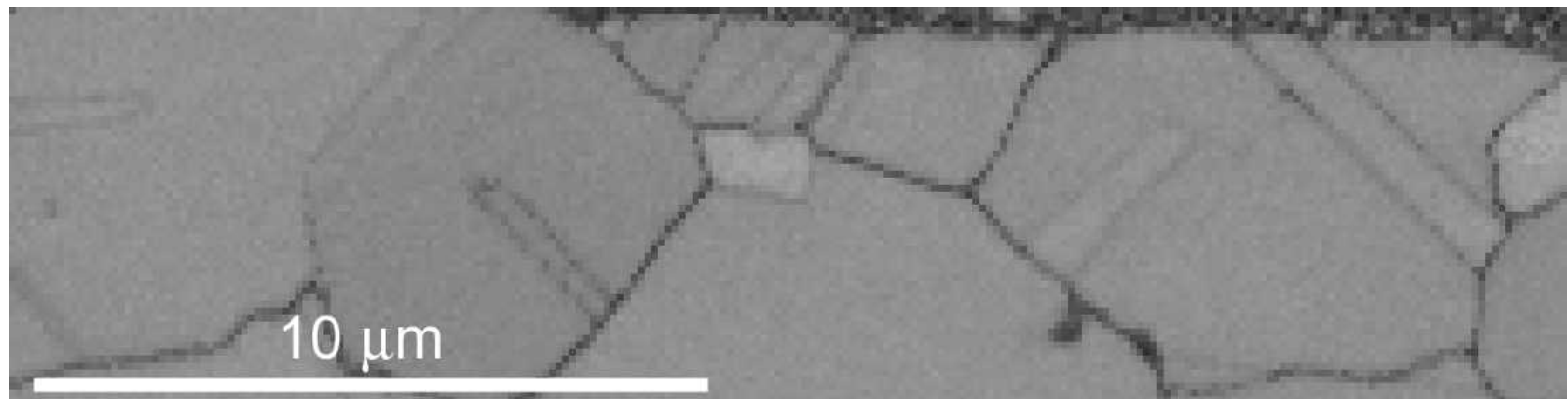
- Selection of alternative alloys with even lower M_s temperatures. Keep M_s below room temperature, even with depletion of Cr and other elements.
- Candidate alloys: 21-6-9 (Nitronic 40) and 22-13-5 (Nitronic 50)



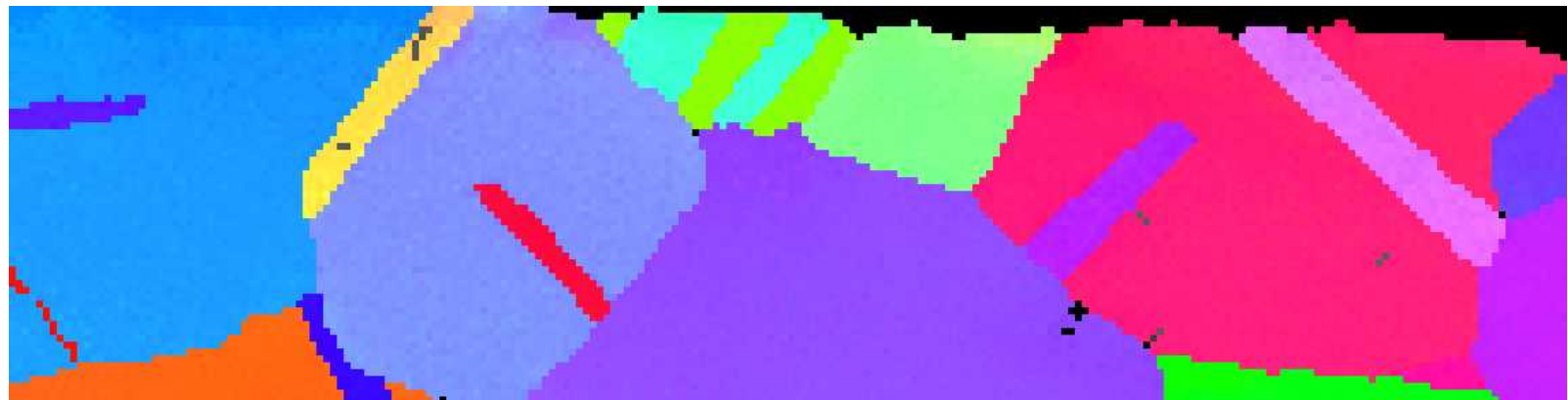
- “Simulated” alloy depletion profiles for Nitronic 40 and Nitronic 50.
- Calculated M_s temperatures are significantly lower than 304L.



Nitronic 50 Results: *No bcc formation at the surface after pre-oxidation and GTM sealing*



Band Contrast image

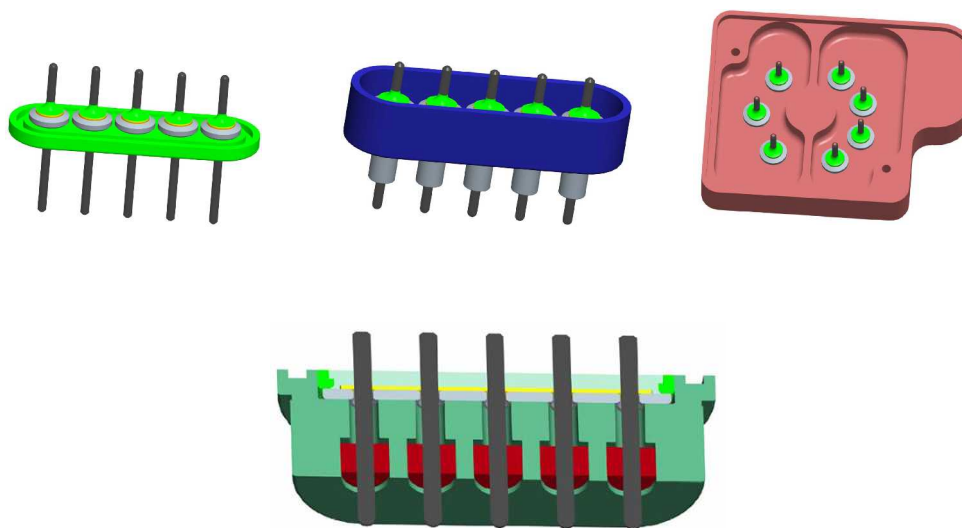


Austenite

- The layer morphology and the continuous composition profile (no step) suggested it was formed by martensitic mechanism. Thermochemical modeling supported a martensitic reaction and discounted a diffusional transformation.
- Good correlations, in terms of bulk M_s and the effect of alloy depletion on M_s , were found using the Eichelman and Hull equation. M_s temperatures at or near room temperature are possible in the alloy-depletion zone at the surface of 304L.
- Alternative austenitic alloys, in particular Nitronic 50, are promising candidates to eliminate bcc layer formation at the glass/metal interface.



3. Glass/Metal and Glass-Ceramic/Metal Seals to Electrical Contact Pins

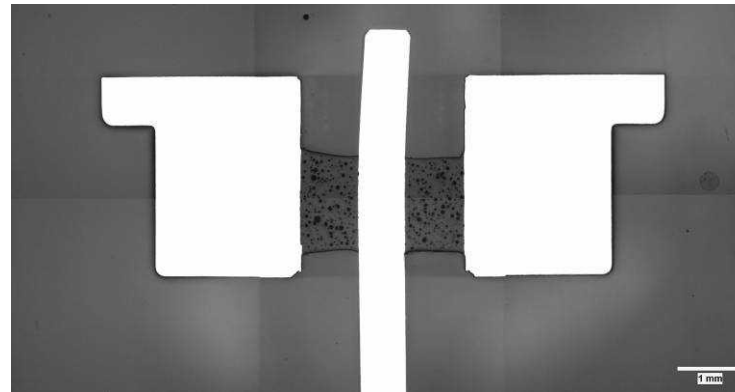




Contact Pin Materials

- Low expansion Ni-Fe alloys such as Alloy 52 for *matched seals*
- Precious metal contact alloys for low contact resistance, corrosion resistance, and high hardness/wear properties
 - Paliney 7: 35Pd-30Ag-14Cu-10Au-10Pt-1.0Zn

Paliney is trademark of Deringer-Ney Inc.,
Bloomfield, CT

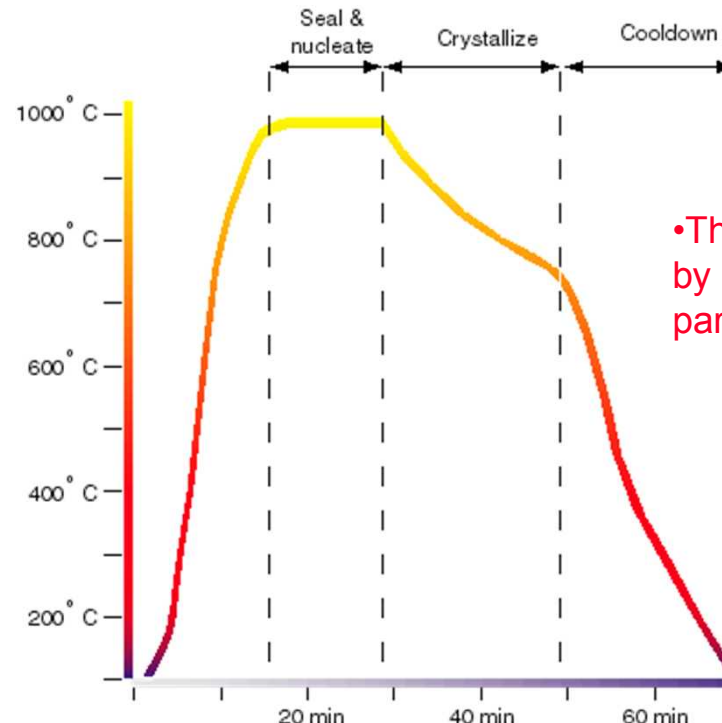
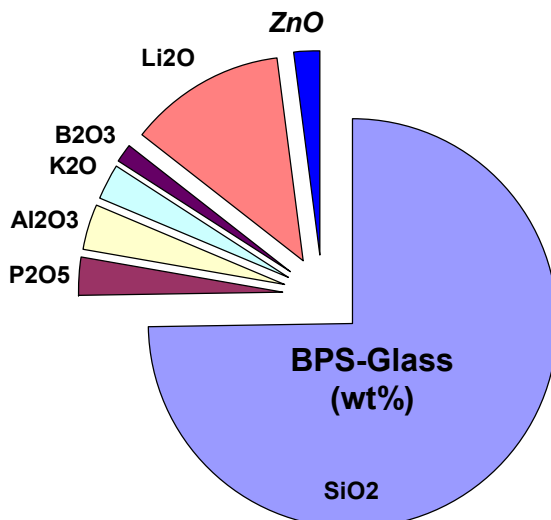


Materials Set

BPS Glass-Ceramic, 304L stainless steel shell, Paliney 7 pin

- **BPS (Belt Processable S-glass)**
 - Patented by Sandia (Scott Reed, Ron Stone, Howard McCollister, Paul Wengert; US patent #: 5,820,989)
 - Designed to be processed utilizing belt rather than batch furnace
 - Crystalline assemblage similar to S/SB after heat treatment
 - Cristobalite, Quartz, Li-metasilicate, Li-disilicate, Li-phosphate

Composition of BPS glass-ceramic



- The CTE of BPS can be altered by tailoring crystallization of parent glass
 - Higher degree of crystallization → higher CTE



Low hardness was observed in some Paliney-7 heat lots after BPS glass-ceramic processing

Hardness requirements: minimum 300 Knoop (100g load)

Thermal Profile	Paliney 7 Pin Hardness (Knoop Hardness)
RT to 1000C @ 25C/min; hold 12min; to 660C @ 6C/min; 0min hold; to 482C @ 25C/min with 45 min hold; to RT @ 5 C/min	Rod 293 / 307
RT to 1000C @ 25C/min; hold 12min; to 660C @ 6C/min; 0min hold; to 482C @ 25C/min with 45 min hold; to RT @ 5 C/min	Rod 298 / 302
RT to 1000C @ 25C/min; hold 12min; to 660C @ 6C/min; 0min hold; to 482C @ 25C/min with 45 min hold; to RT @ 5 C/min	Wire 259

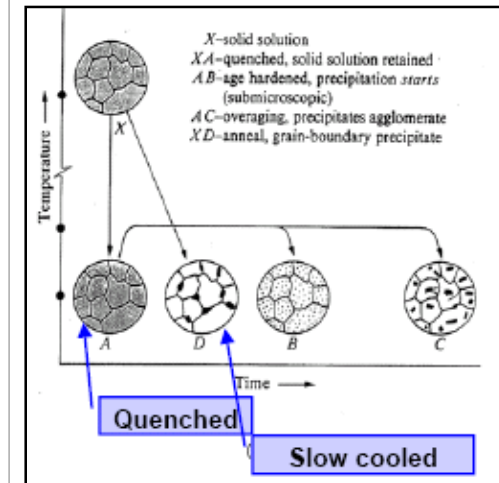
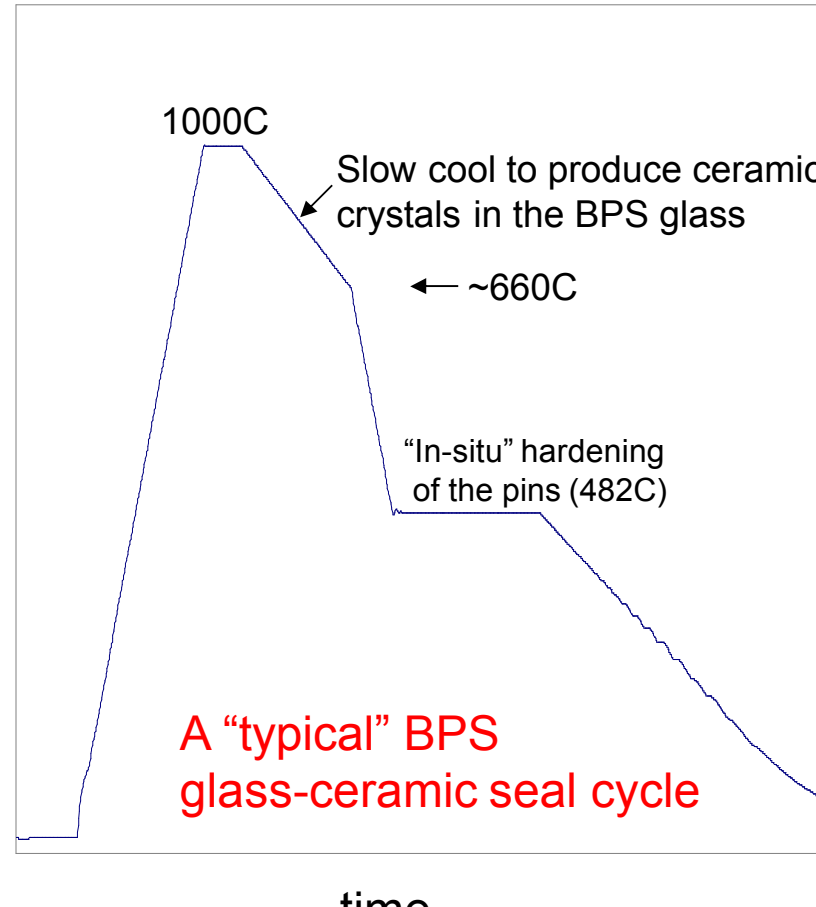
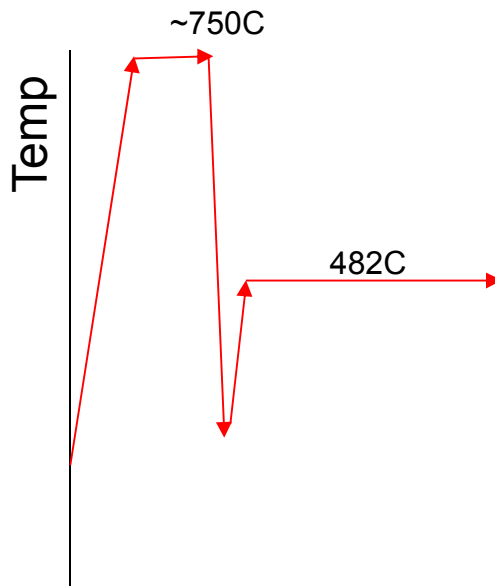
Melt #	Composition (wt.%)							
	Ag	Zn	Pd	Cu	Ni	Au	Fe	Pt
W34680W (wire)	30.39	0.97	34.82	14.09	0.02	10.00	0.01	9.84
W43004W (rod)	30.07	0.94	34.86	13.88	<.0014	9.98	<.0024	9.83

- No apparent difference in the bulk chemistry of the heats

- “Rod” vs. “wire”: processed the same except that rod is “batch annealed” (short lengths are heat treated in a batch oven) and wire is “strand annealed” (continuous feedthrough of wire through an oven)
- Glass sealing process at 1000°C should remove any prior effects of the wire or rod making process
- However, minor differences in chemistry, not shown in the melt cert., could affect the precipitation hardening process and the final hardness after glass sealing

Glass-ceramic sealing cycle: Slow-cooling through the apparent Paliney-7 PPt. Solvs Range

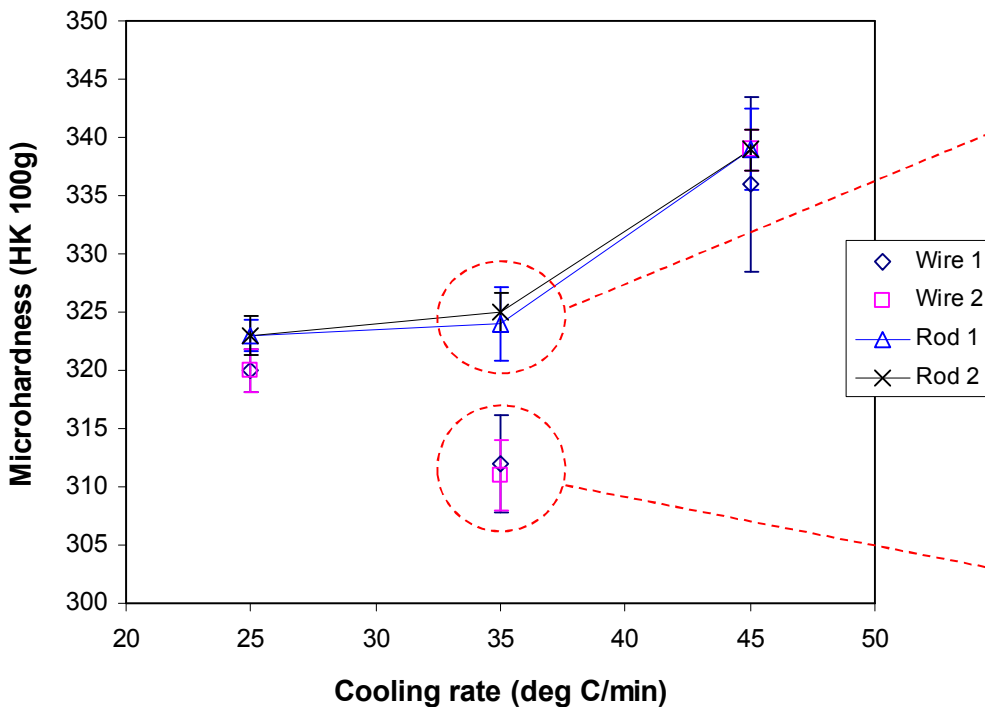
Ideal precipitation-hardening process



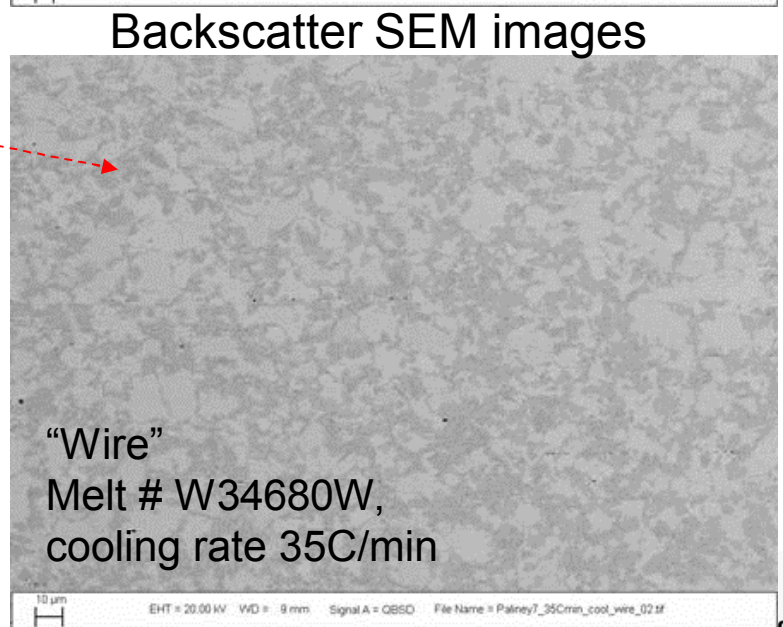
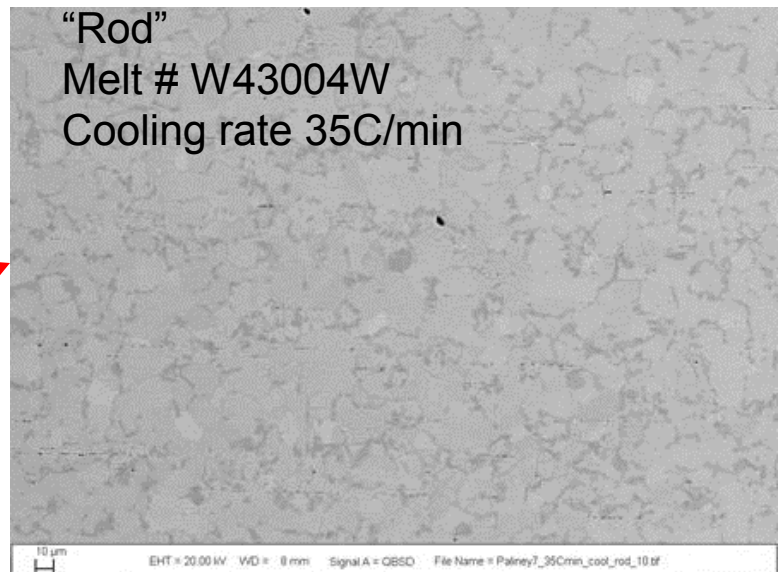
- The slow-cooling rate and long time spent at high temperatures are the likely causes of reduced hardness
- Original thermal profile was slow-cool to 660C, then faster cool to 482C

Initial Cooling Rate Study: Some Hardness and Microstructural Differences Observed Between Paliney-7 Heats

- Paliney-7 pin samples heated to 1000°C and cooled at 25, 35, and 45C/min

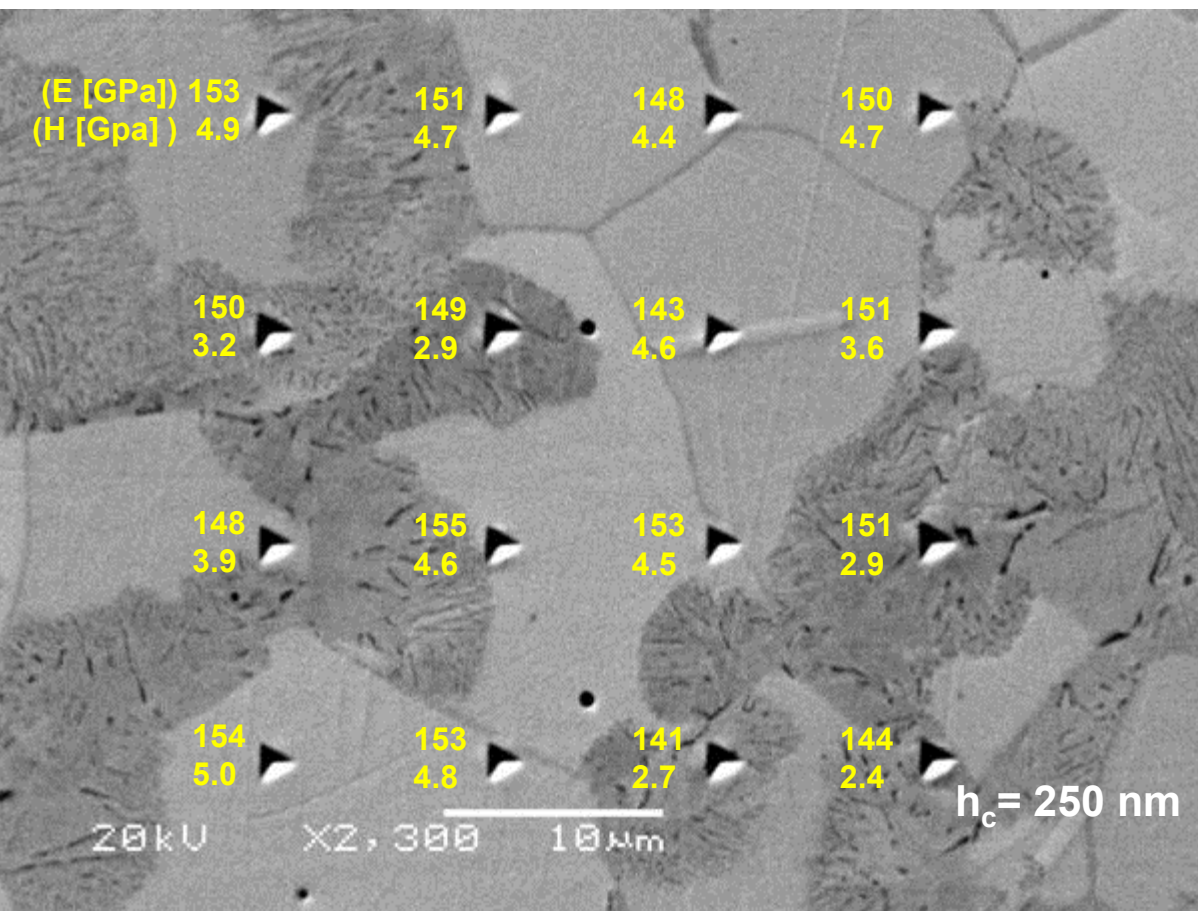


- Some differences observed between rod and wire, although inconsistent with cooling rate
- Backscatter SEM microscopy revealed a multiphase Paliney microstructure



Nano-Indentation Results: Dark 2-phase Regions are Softer than the Matrix Grains

- Indent array covers different microstructural regions of the sample



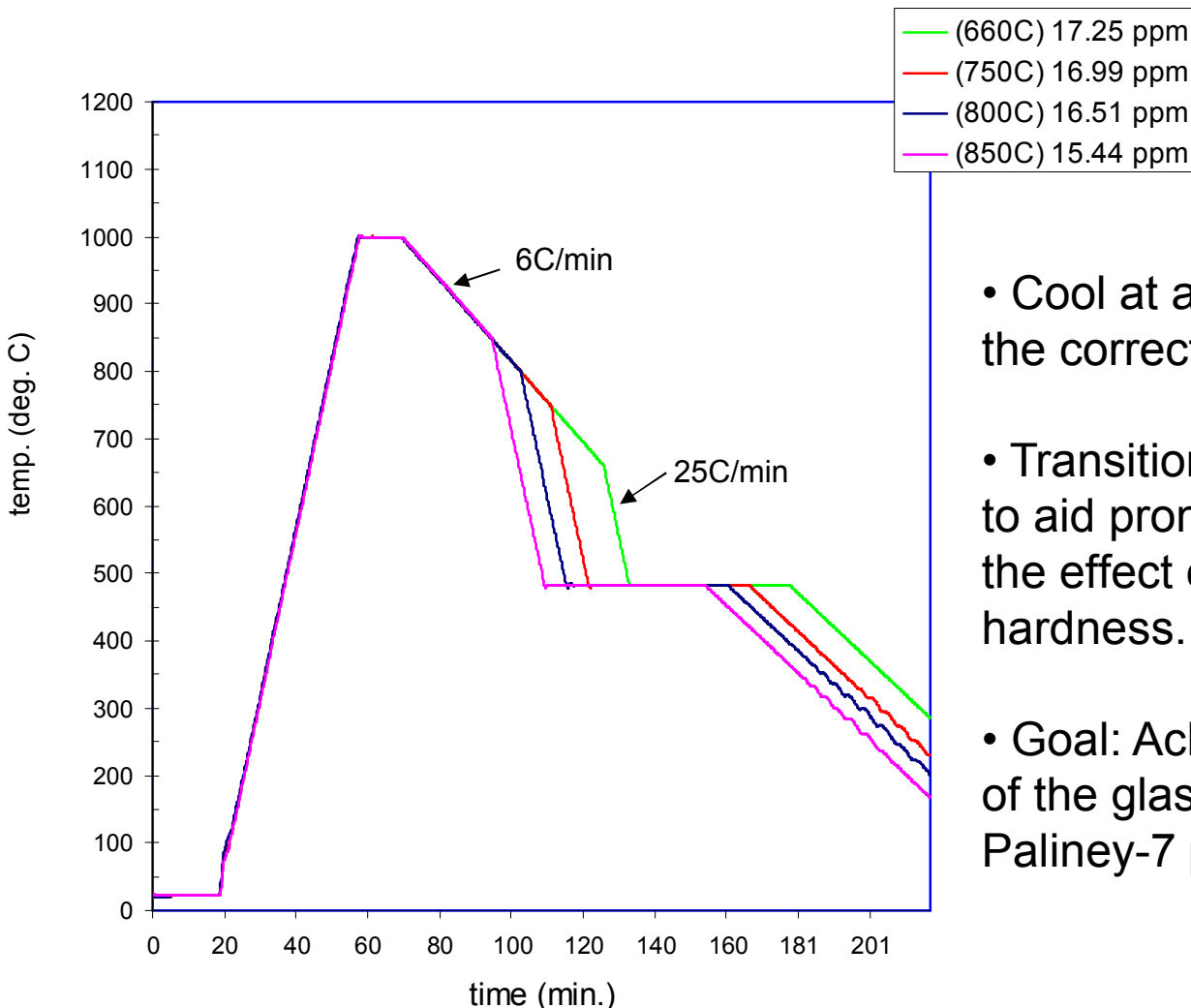
“Wire”
Melt # W34680W,
cooling rate 35C/min

$E_{avg} = 150 \pm 4$ GPa
 E (as per ASTM B540)= 117 GPa
•Discrepancy possibly due to indent
‘pile-up’

$H_{light} = 4.5 \pm 0.4$ GPa
 $H_{dark} = 2.8 \pm 0.2$ GPa

Bulk H (ASTM B540)= 3.2-3.9 GPa

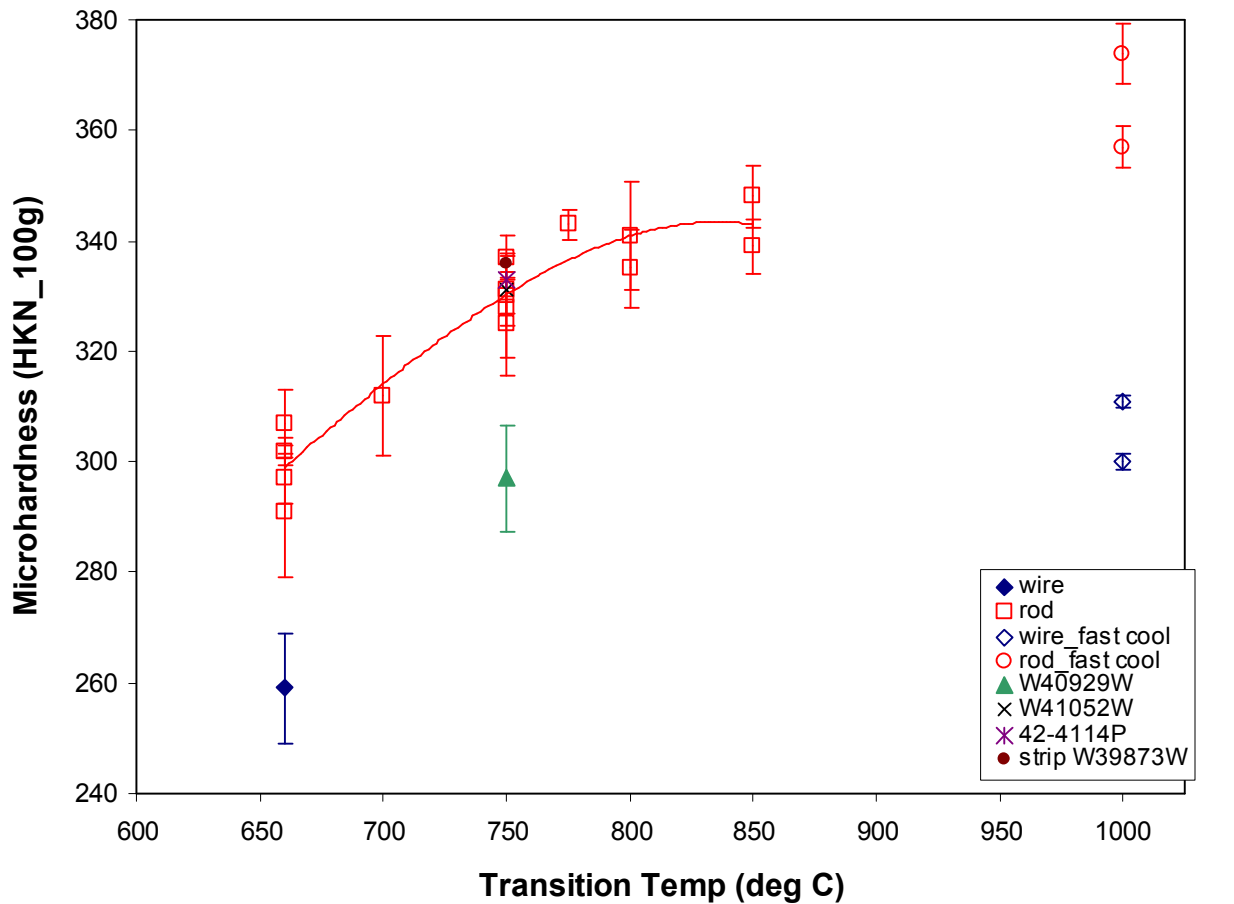
Cooling-Rate “Transition” Study



- Cool at a slow rate initially to achieve the correct CTE of the glass-ceramic
- Transition to a faster cooling rate to aid promote pin hardening. Analyze the effect of this transition temp. on pin hardness.
- Goal: Achieve both the desired CTE of the glass-ceramic and high Paliney-7 pin hardness

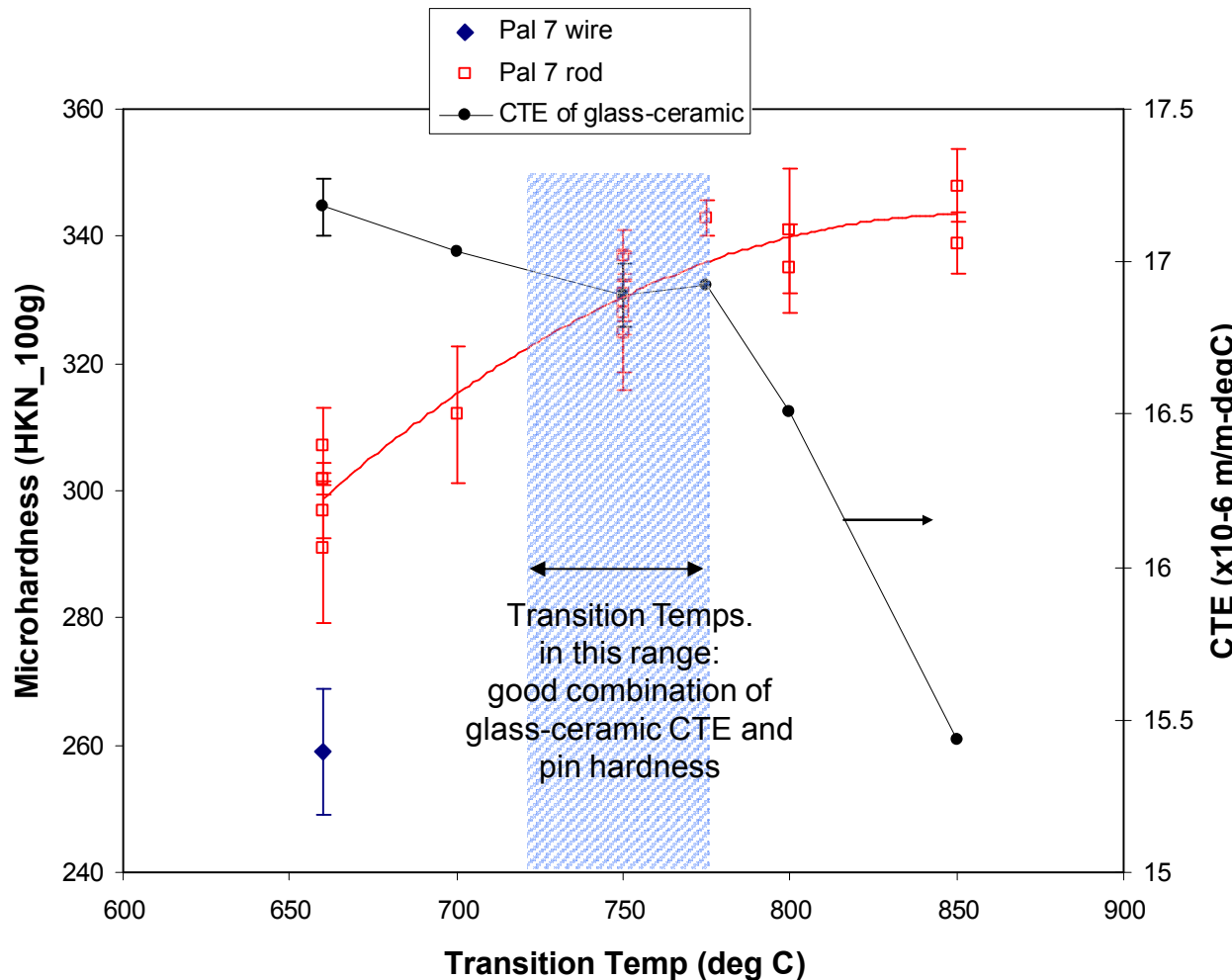


Results: Consistent Trend of Increasing Pin Hardness with Increasing “Cooling Rate Transition Temp.”



A Processing Window can be Developed for both Glass-Ceramic CTE and Pin Hardness

- Superimpose CTE and Pin Hardness Results



What causes low hardness values?: Discontinuous Precipitation (DP) (or discontinuous coarsening (DC))

- Precipitation of a 2-phase lamellar structure behind a moving grain boundary
- Coarse precipitate structure is generally detrimental to mechanical properties
- Confirmed by electron backscatter diffraction (EBSD)

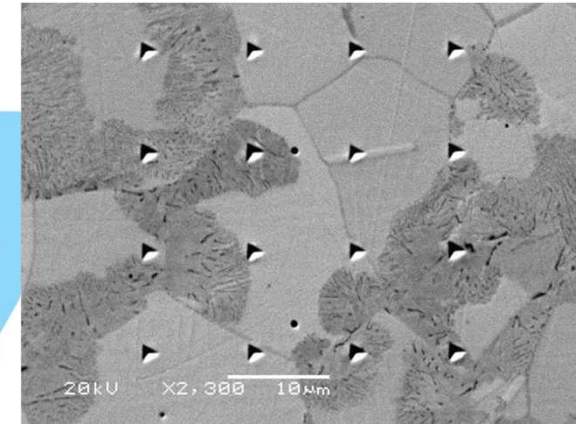
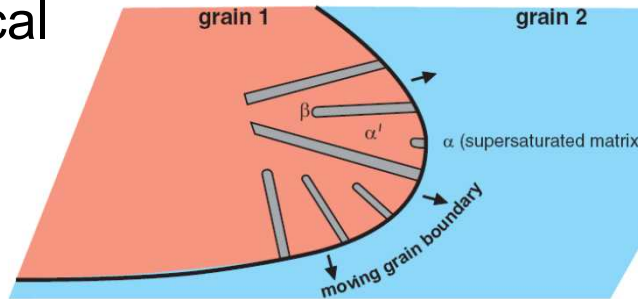
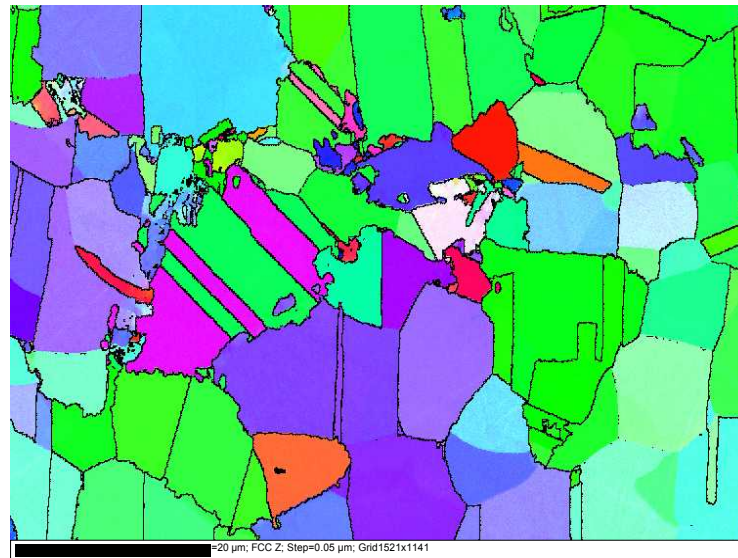
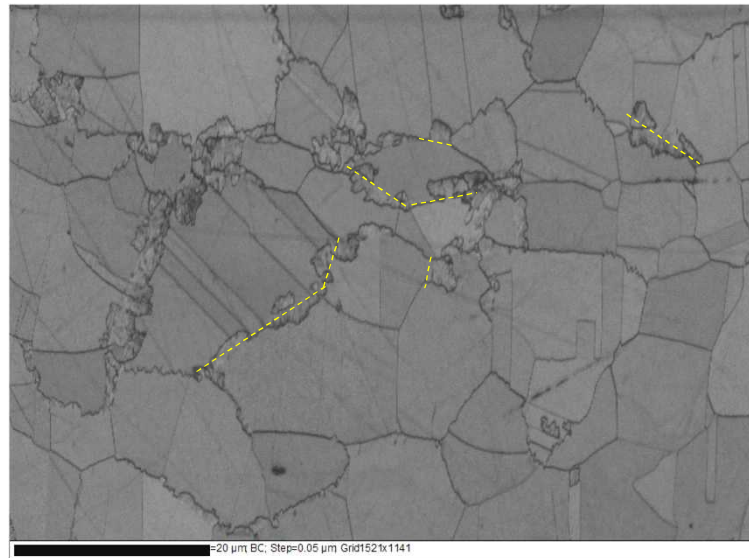
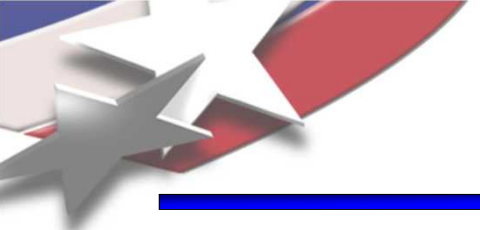


Fig. 1 Schematic of discontinuous precipitation, $\alpha \rightarrow \alpha' + \beta$





Summary

The high temperatures and furnace environments involved in glass/metal sealing can induce significant metallurgical effects on the metallic component of the joint:

- Pre-oxidation of stainless steels is affected by subtle changes in alloy chemistry.
- The composition and morphology of the pre-oxidized layer greatly affects the glass/metal seal robustness.
- Surface alloy depletion and a martensitic phase transformation can be induced in stainless steels during pre-oxidation and glass sealing.
- Alternative candidate alloys show promise for replacing 304L.
- Detrimental low hardness in Pal-7 was found to be due to discontinuous precipitation. A processing window was found by limiting the time at high temperature -- changing to a fast cooling rate early in the process.

